Supporting Information

Noble metal-free triphenylamine-based coordination capsule with NADH mimics as a renewable vessel for enhanced biomimetic hydrogenation

Huali Wang,[†a] Bangzhou Xing,[†a] Shuaiwei Wang,[a] Yu Zhang,[a] Jing Wang,[a] Liang Zhao,[*a] and Chunying Duan[b]

[a]State Key Laboratory of Fine Chemicals, Frontier Science Center for Smart Materials, School of Chemical Engineering, Dalian University of Technology, Dalian 116024.

[b]State Key Laboratory of Coordination Chemistry, Nanjing University, Nanjing 210093.

[†]These authors contributed equally to this work.

*Corresponding Author Email: zhaol@dlut.edu.cn

Contents

1. Experimental Section

All the chemicals and solvents were of reagent-grade quality obtained from commercial sources and used without further purification. Zn−**ZPB** was synthesized according to the published procedure.[S1]

The elemental analyses of C, H and N were performed on a Vario EL III elemental analyzer. ^{1}H NMR and ^{13}C NMR spectra were measured on Bruker Avance spectrometer 400 MHz with internal standard TMS at δ 0.0 ppm. ESI-MS were carried out on an Agilent 6224 HPLC-TOF spectrometer using methanol as mobile phase. UV-Vis spectra were collected on a HP 8453 spectrometer. The solution fluorescent spectra were measured on Edinburgh FS 920. Cyclic voltammetry experiments were conducted in a solution containing 0.1 M n-Bu_4NPF_6 electrolyte, using a freshly polished glassy carbon electrode with a diameter of 5 mm as a working electrode, a platinum wire with 0.5 mm diameter as a counter electrode and an Ag/AgCl (3 M KCl) electrode. Isothermal Titration Calorimetry (ITC) experiments were performed by an isothermal titration microcalorimeter at atmospheric pressure and at 298 K, giving the association constants (K_a) and the thermodynamic parameters. The guest in CH_3CN/H_2O (4:1 in v:v, pH = 4.50) was sequentially injected from a 0.250 mL syringe with stirring at 250 rpm into the host solution in the sample cell (1.30 mL volume). All the thermodynamic parameters reported in this work were obtained by using the "independent" model.

Photocatalytic hydrogenation reactions were carried out in a 10 mL flask, varying amounts of the catalyst and substrate in CH_3CN/H_2O (4:1 in v:v) were added to obtain a total volume of 5.0 mL. The pH of this solution was adjusted to a specific pH value by adding H_2SO_4 or NaOH and measured with a pH meter. The flask was sealed with a septum, degassed by bubbling argon for 15 min under atmospheric pressure at room temperature. After that, the samples were irradiated by a LED Lamp, with the reaction temperature maintained at 298 K by using a water filter to absorb heat. ^{1}H NMR spectra were recorded to determine the conversions (using 1,3,5-trimethoxybenzene as an internal standard). The crude product could be purified by column chromatography on silica gel to afford the corresponding products.

2. Preparation and Characterizations

Scheme S1 The synthetic routes of the H_2**ZPD**.[S1]

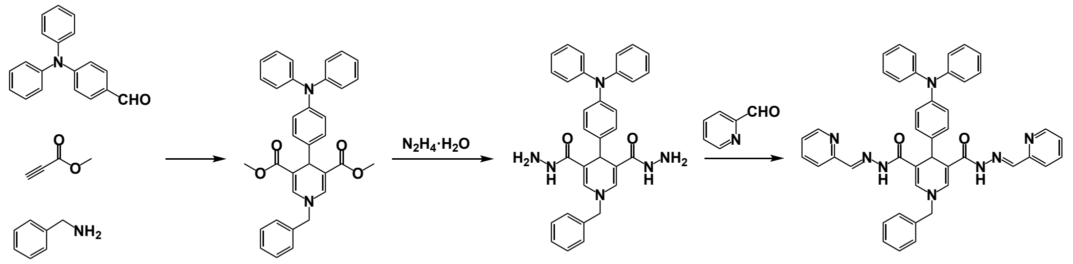

Dimethyl 1-benzyl-4-(4-(diphenylamino)-phenyl)-1,4-dihydropyridine-3,5-dicarboxylate

Methyl propiolate (1.68 g, 20 mmol), 4-(diphenylamino) benzaldehyde (2.73 g, 10 mmol), and benzylamine (1.07 g, 10 mmol) in glacial acetic acid (2.0 mL) were heated at 80°C for 30 min. After cooling, the mixture was poured into water (20 mL) and stirred for 1 h. The solid product was filtered and washed with Et_2O (10 mL×3) to give pure dimethyl 1-benzyl-4-(4-(diphenylamino)-phenyl)-1,4-dihydropyridine-3,5-dicarboxy-late, which was recrystallized by ethanol. Yield: 2.77 g, 52.3%. **^{1}H NMR** (400 MHz, DMSO-d_6, *ppm*): δ 7.50 (s, 2H), 7.41-7.37 (m, 2H), 7.35-7.33 (m, 2H), 7.30-7.26 (m, 5H), 7.05-6.99 (m, 4H), 6.96-6.93 (m, 4H), 6.82-6.80 (m, 2H), 4.80 (s, 2H), 4.69 (s, 1H), 3.58 (s, 6H). **^{13}C NMR** (101 MHz, DMSO-d_6, *ppm*): δ 191.04, 166.64, 147.60, 135.07, 131.46, 130.51, 129.97, 126.88, 124.75, 124.43, 123.61, 123.26, 120.29, 118.64, 117.33, 111.12, 51.97, 36.69.

1-benzyl-4-(4-(diphenylamino)-phenyl)-1,4-dihydropyridine-3,5-dicarbohydrazide

A mixture solution of 80% hydrazine hydrate (50 mL) and dimethyl 1-benzyl-4-(4-(diphenylamino)-phenyl)-1,4-dihydropyridine-3,5-dicarboxylate (5.30 g, 10 mmol) was stirred at 85°C for 24 h. The white precipitate was formed, which was collected by filtration, washed with methanol and dried in vacuum. Yield: 2.63 g, 49.7%. **^{1}H NMR** (400 MHz, DMSO-d_6, *ppm*): δ 8.72 (s, 2H), 7.39-7.25 (m, 9H), 7.22 (s, 2H), 7.08-7.06 (d, 2H), 7.03-6.99 (m, 2H), 6.94-6.92 (m, 4H), 6.80-6.78 (d, 2H), 4.97 (s,1H), 4.60 (s, 2H), 4.17 (s, 4H). **^{13}C NMR** (101 MHz, DMSO-d_6, *ppm*): δ 166.62, 147.25, 145.07, 141.18, 137.81, 133.83, 129.41, 128.64, 128.46, 127.65, 127.54, 123.49, 123.29, 122.67, 108.39, 56.85, 34.48.

Preparation of H_2**ZPD**

1-benzyl-4-(4-(diphenylamino)-phenyl)-1,4-dihydropyridine-3,5-dicarbohydrazide (5.30 g, 10 mmol) was added to a ethanol solution (50 mL) containing 2-pyridylaldehyde (2.35 g, 22 mmol). After 5 drops of acetic acid was added, the mixture was heated at 85°C under magnetic stirring for 12 h. The yellow solid was collected by filtration, washed with methanol and dried in vacuum. Yield: 5.35 g, 75.5%. **^{1}H NMR** (400 MHz, DMSO-d_6, *ppm*): δ 11.41 (s, 2H), 8.59-8.58 (d, 2H), 8.25 (s, 2H), 7.84 (d, 4H), 7.53 (s, 2H), 7.43-7.32 (m, 7H),7.26-7.23 (m, 4H), 7.18-7.16 (d, 2H), 7.00-6.97 (m, 2H), 6.94-6.92 (d, 4H), 6.86-6.84 (d, 2H), 5.30 (s, 1H), 4.77 (s, 2H). **^{13}C NMR** (101 MHz, DMSO-d_6, *ppm*) δ: 164.42, 153.99, 149.90, 147.71, 145.82, 145.72, 141.59, 138.16, 137.18, 136.13, 129.92, 129.08, 129.08, 128.28, 127.74, 124.46, 124.10, 123.71, 123.22, 120.03, 109.40, 57.66, 35.69. **Elemental analysis** calcd for $C_{44}H_{36}N_8O_2$: H, 5.12%; C, 74.56%; N, 15.81%; Found: H, 5.09%; C, 74.49%; N, 15.77%. **ESI-MS**: calcd for $C_{44}H_{36}N_8O_2$ 708.30, found 709.31 $[M+H]^+$.

Preparation of Zn−**ZPD**

$Zn(ClO_4)_2{\cdot}6H_2O$ (37.2 mg, 0.10 mmol) and H_2**ZPD** (70.8 mg, 0.10 mmol) were dissolved in CH_3OH/DMF (2:1 in volume) to give a yellow solution The solution was left for several weeks at room temperature to give X-ray quality yellow block crystals. Yield: 37.4%. **^{1}H NMR** (400 MHz, DMSO-d_6, *ppm*): δ 11.56 (s, 1H), 8.57 (d, 2H), 8.28 (s, 2H), 7.88 (d, 4H), 7.59 (s, 2H), 7.43-7.34 (m, 7H), 7.27-7.23 (m, 4H), 7.17-7.15 (d, 2H), 7.01-6.98 (m, 2H), 6.93-6.91 (d, 4H), 6.84-6.83 (d, 2H), 5.39 (s, 1H), 4.80 (s, 2H). **Elemental analysis** calcd for $Zn_4C_{176}H_{136}Cl_4N_{32}O_{24}{\cdot}CH_3OH$: H, 3.83%; C, 58.08%; N, 12.25%; Found: H, 3.71%; C, 58.22%; N, 12.36%. **ESI-MS:** *m/z*: 1030.6188 $[H_3Zn_4(\mathbf{ZPD})_4]^{3+}$, 1063.9370 $[H_4Zn_4(\mathbf{ZPD})_4{\cdot}ClO_4]^{3+}$, 1097.2567 $[H_5Zn_4(\mathbf{ZPD})_4{\cdot}2ClO_4]^{3+}$, 1545.4228 $[H_2Zn_4(\mathbf{ZPD})_4]^{2+}$, 1595.4027 $[H_3Zn_4(\mathbf{ZPD})_4{\cdot}ClO_4]^{2+}$, and 1645.3811 $[H_4Zn_4(\mathbf{ZPD})_4{\cdot}2ClO_4]^{2+}$.

Scheme S2 The synthetic route of benzoxazinones.[S2]

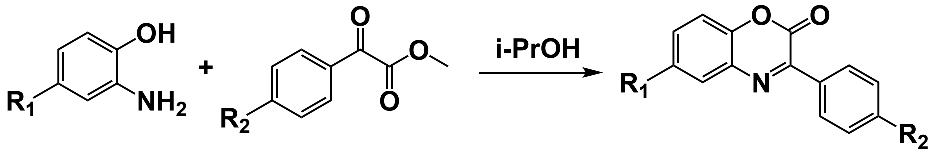

Methyl phenylglyoxylate (1.5 mmol) and 2-Aminophenol (1.0 mmol) was added to 10 mL of i-PrOH, the mixture was reflux overnight under magnetic stirring for 12 h. After the reaction, the precipitate was filtered and washed with i-PrOH to obtain pure benzoxazinone compounds.

3. Single Crystal X-ray Crystallography

Intensity of the Zn−**ZPD** was collected on a Bruker SMART APEX CCD diffractometer with graphite-monochromated Mo-Kα (λ = 0.71073 Å) radiation source; the data were using the SMART and SAINT programs.[S3,S4] The structure was solved by Intrinsic Phasing using SHELXT and refined by Least Squares minimization using SHELXL in OLEX2.[S5−S7] Non-H atoms were refined with anisotropic displacement parameters. Hydrogen atoms in the backbones were fixed geometrically at calculated distances and allowed to ride on the parent non-hydrogen atoms, whereas some of the disordered solvent molecules were not treated during the structural refinements. The SQUEEZE program was carried out for Zn−**ZPD**.[S8]

Table S1. Crystallographic data for Zn−**ZPD.**

Compound	Zn−**ZPD**
Formula	$Zn_4C_{176}H_{136}Cl_4N_{32}O_{24}$
M (g·mol^{-1})	3486.44
Crystal system	Tetragonal
Space group	I-4
a (Å)	20.750(3)
b (Å)	20.750(3)
c (Å)	28.402(4)
V (Å^3)	12228(3)
Z	2
D_{calcd} (g·cm^{-3})	0.947
F (000)	3592
μ (mm^{-1})	0.485
T (K)	219
Refl. collected/unique	136340/10989 [R_{int} = 0.2083]
R_1 [$I > 2\sigma(I)$]	0.0821
wR_2 (all data)	0.3188
Goodness of fit	0.992
Max/min Δρ(e Å^{-3})	0.570 and −0.272
CCDC Number	2416930

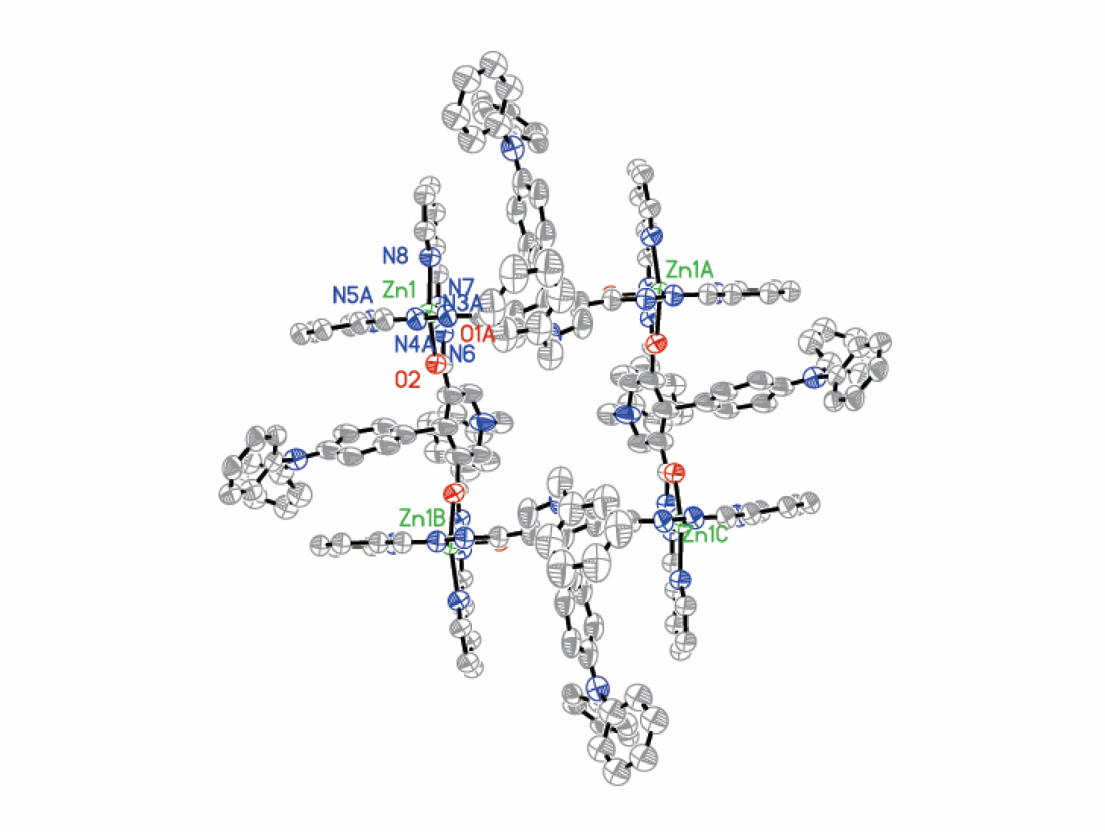

Figure S1. An ORTEP plot of the Zn−**ZPD**, showing 30% probability displacement ellipsoids of non-hydrogen atoms. Hydrogen atoms are omitted for clarity.

Table S2. Selective bond distance (Å) in Zn−**ZPD**

Bond	Bond length/Å	Bond	Bond length/Å
Zn1-O2	2.090(9)	C32-C21	1.475(17)
Zn1-N4	2.198(14)	C33-C34	1.390(17)
Zn1-O1	2.086(10)	N7-N6	1.303(14)
Zn1-N7	2.099(13)	N7-C40	1.316(15)
Zn1-N5	2.162(11)	C26-C25	1.539(18)
Zn1-N8	2.145(6)	C40-C41	1.416(16)
Cl1-O5	1.459(10)	C16-C20	1.64(2)
Cl1-O3	1.427(10)	N2-C25	1.422(15)
Cl1-O4	1.451(11)	N1-C3	1.378(12)
Cl1-O13	1.419(10	N1-C11	1.445(13)
O2-C39	1.327(16)	N3-C32	1.407(19)
N4-N3	1.401(16)	N3-C32	1.407(19)
N4-C33	1.200(16)	C18-C17	1.45(2)
O1-C32	1.300(19)	C17-C16	1.314(19)
C39-N6	1.383(17)	C15-C16	1.36(2)
C39-C24	1.379(16)	C15-C14	1.52(2)
C19-N1	1.35(2)	C19-C14	1.48(2)
C19-C18	1.38(2)		

Table S3. Selective bond angle (°) in Zn−**ZPD**

Bond	Bond angle/°	Bond	Bond angle/°
O2-Zn1-N4	107.6(4)	C22-N2-C25	115.9(9)
O2-Zn1-N5	90.4(17)	C23-N2-C25	124.0(9)
O2-Zn1-N8	151.0(4)	C27-C26-C25	121.3(13)
O1-Zn1-O2	91.2(4)	C31-C26-C25	118.5(13)
O1-Zn1-N4	76.8(5)	C39-C24-C20	122.5(10)
O1-Zn1-N7	105.8(4)	C39-C24-C23	116.2(9)
O1-Zn1-N5	150.8(19)	N7-C40-C41	115.6(14)
O1-Zn1-N8	92.9(3)	C42-C41-C40	122.8(9)
N7-Zn1-O2	75.1(4)	N8-C41-C40	117.1(9)
N7-Zn1-N4	176.4(5)	C41-N8-Zn1	112.8(5)
N7-Zn1-N5	102.8(19)	C45-N8-Zn1	127.1(5)
N7-Zn1-N8	76.2(4)	N2-C25-C26	115.0(14)
N5-Zn1-N4	74.9(19)	N1-C19-C14	122(2)
N8-Zn1-N4	101.2(4)	C18-C19-C14	115.6(19)
N8-Zn1-N5	99.6(16)	C19-N1-C3	123.3(12)
O3-Cl1-O5	116.2(11)	C19-N1-C11	120.4(12)
O3-Cl1-O4	105.7(10)	C3-N1-C11	116.0(11)
O3-Cl1-O13	120.0(11)	C16-C15-C14	120.2(16)
O4-Cl1-O5	106.8(11)	O1-C32-N3	123.1(15)
O13-Cl1-O5	106.2(10)	O1-C32-C21	118.8(14)
O13-Cl1-O4	99.9(10)	N3-C32-C21	118.1(16)
C39-O2-Zn1	116.6(9)	O2-C39-C24	120.4(13)
N3-N4-Zn1	112.1(9)	C24-C39-N6	124.7(15)
C33-N4-Zn1	115.3(13)	N1-C19-C18	122.3(15)
C33-N4-N3	131.7(16)	N4-N3-C32	112.5(14)
C32-O1-Zn1	114.5(10)	C19-C18-C17	120.6(17)
O2-C39-N6	114.9(14)	C16-C17-C18	125(2)

N6-N7-C40	126.4(14)	C10-C11-N1	118.2(10)
C40-N7-Zn1	118.0(11)	C12-C11-N1	121.7(10)
C35-C34-C33	122.3(10)	N7-N6-C39	117.9(13)
N5-C34-C33	117.7(10)	C19-C14-C15	118.6(18)
C34-N5-Zn1	111.0(6)	N1-C3-C2	120.7(10)
C38-N5-Zn1	128.9(6)	N1-C3-C4	119.1(10)
C17-C16-C15	119(2)	C24-C20-C16	109.5(9)
C17-C16-C20	125.8(19)	C20-C21-C32	122.9(9)
C15-C16-C20	115.5(14)	C22-C21-C32	116.7(9)
C21-C20-C16	106.3(8)	N4-C33-C34	120.2(17)
N6-N7-Zn1	115.6(9)		

4. Studies of Host−Guest Interaction

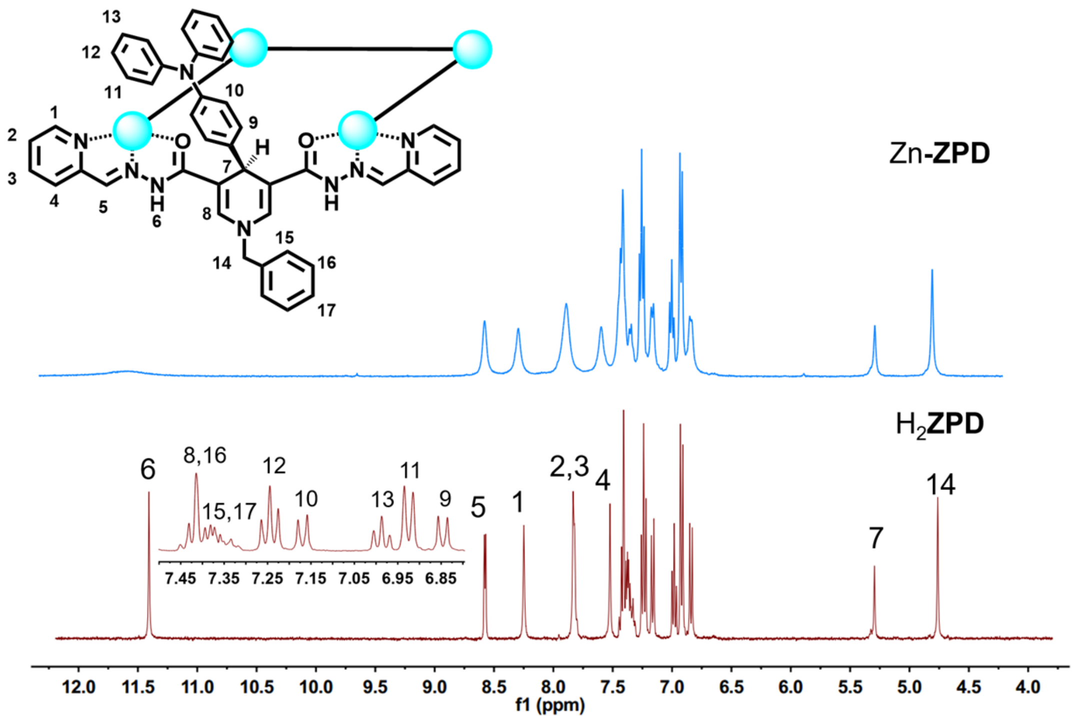

Figure S2. ^{1}H NMR spectra of H_2**ZPD** and Zn−**ZPD**. The ^{1}H NMR shift and peak width of the Zn−**ZPD** showed significant changes compared to that of the ligand H_2**ZPD**. The disappearance of the imine proton C(O)–NH signal at 11.40 ppm and the slight shift of the tertiary carbon protons (N=CH) and pyridine ring protons indicated the coordination of the ligands to metal ions.

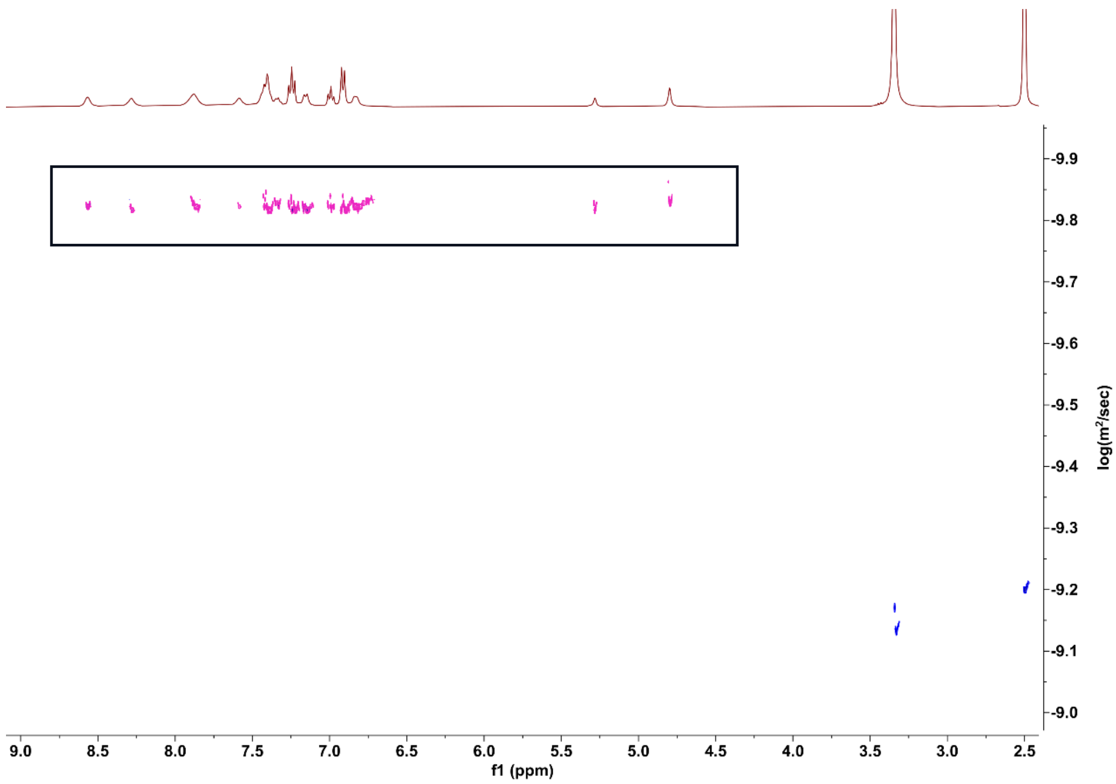

Figure S3. ^{1}H DOSY NMR spectrum of Zn−**ZPD** (0.1 mM) in DMSO-d_6 (diffusion coefficient $D = 1.5\times10^{-10}$ $m^2\cdot s^{-1}$).

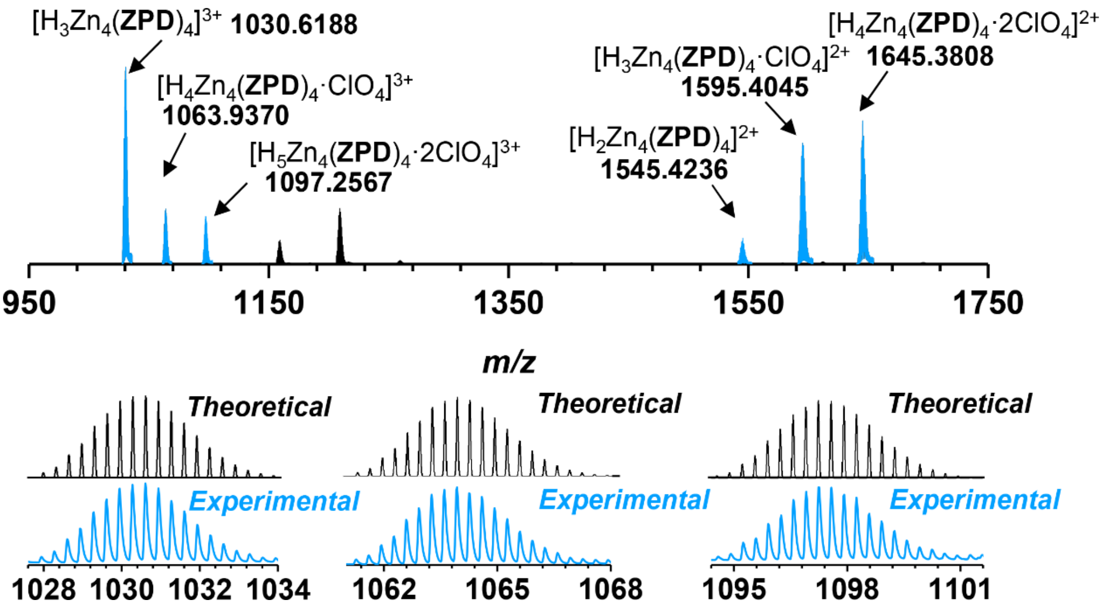

Peak	Value of *m/z*	Species assigned
1	1030.6188	$[H_3Zn_4(\mathbf{ZPD})_4]^{3+}$
2	1063.9370	$[H_4Zn_4(\mathbf{ZPD})_4{\cdot}ClO_4]^{3+}$
3	1097.2567	$[H_5Zn_4(\mathbf{ZPD})_4{\cdot}2ClO_4]^{3+}$
4	1545.4236	$[H_2Zn_4(\mathbf{ZPD})_4]^{2+}$
5	1595.4045	$[H_3Zn_4(\mathbf{ZPD})_4{\cdot}ClO_4]^{2+}$
6	1645.3808	$[H_4Zn_4(\mathbf{ZPD})_4{\cdot}2ClO_4]^{2+}$

Figure S4. ESI-MS of Zn−**ZPD** (0.1 mM) in CH_3CN. The insets showed the theoretical and experimental isotopic patterns at *m/z* = 1030.6188, 1063.9370, and 1097.2567, respectively.

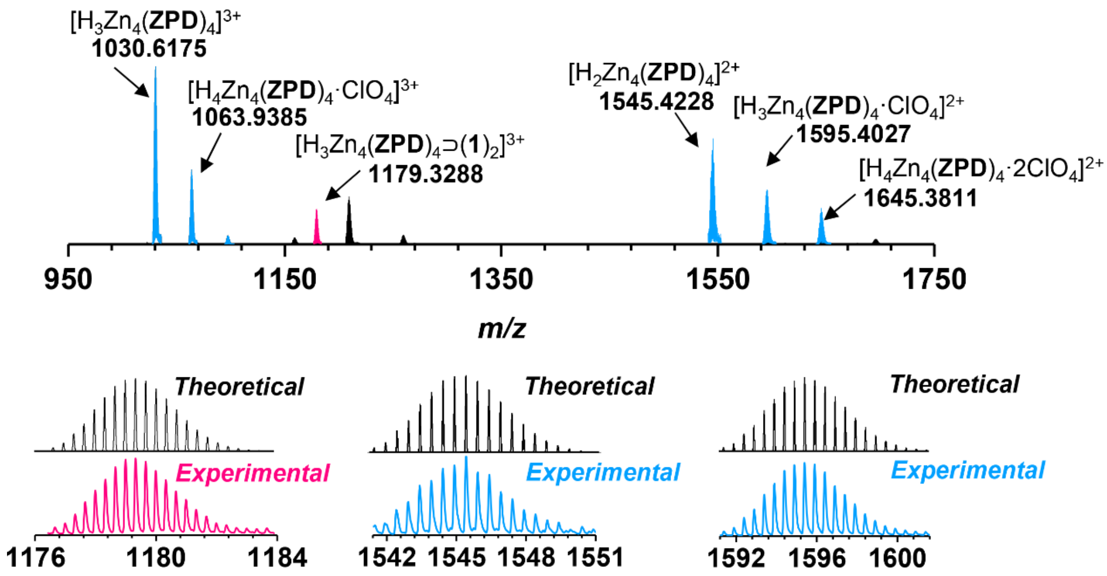

Peak	Value of *m/z*	Species assigned
1	1030.6175	$[H_3Zn_4(\mathbf{ZPD})_4]^{3+}$
2	1063.9385	$[H_4Zn_4(\mathbf{ZPD})_4\cdot ClO_4]^{3+}$
3	1179.3288	$[H_3Zn_4(\mathbf{ZPD})_4\supset(\mathbf{1})_2]^{3+}$
4	1545.4228	$[H_2Zn_4(\mathbf{ZPD})_4]^{2+}$
5	1595.4027	$[H_3Zn_4(\mathbf{ZPD})_4\cdot ClO_4]^{2+}$
6	1645.3811	$[H_4Zn_4(\mathbf{ZPD})_4\cdot 2ClO_4]^{2+}$

Figure S5. ESI-MS of Zn−**ZPD** (0.1 mM) following the addition of 10 equiv. of substrate **1** in CH_3CN. The insets showed the theoretical and experimental isotopic patterns at *m/z* = 1179.3288, 1545.4228, and 1595.4027, respectively.

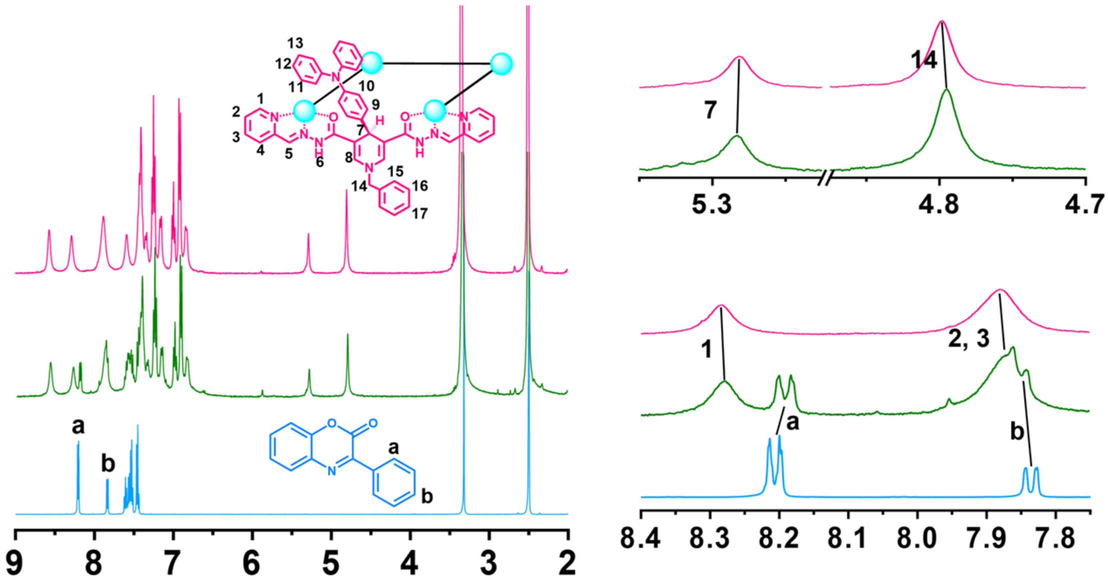

Figure S6. ^{1}H NMR spectra of substrate **1** (0.2 mM, blue line), Zn−**ZPD** (0.1 mM, pink line) and the mixture of Zn−**ZPD** (0.1 mM) with substrate **1** (0.2 mM) in DMSO-d_6 (green line).

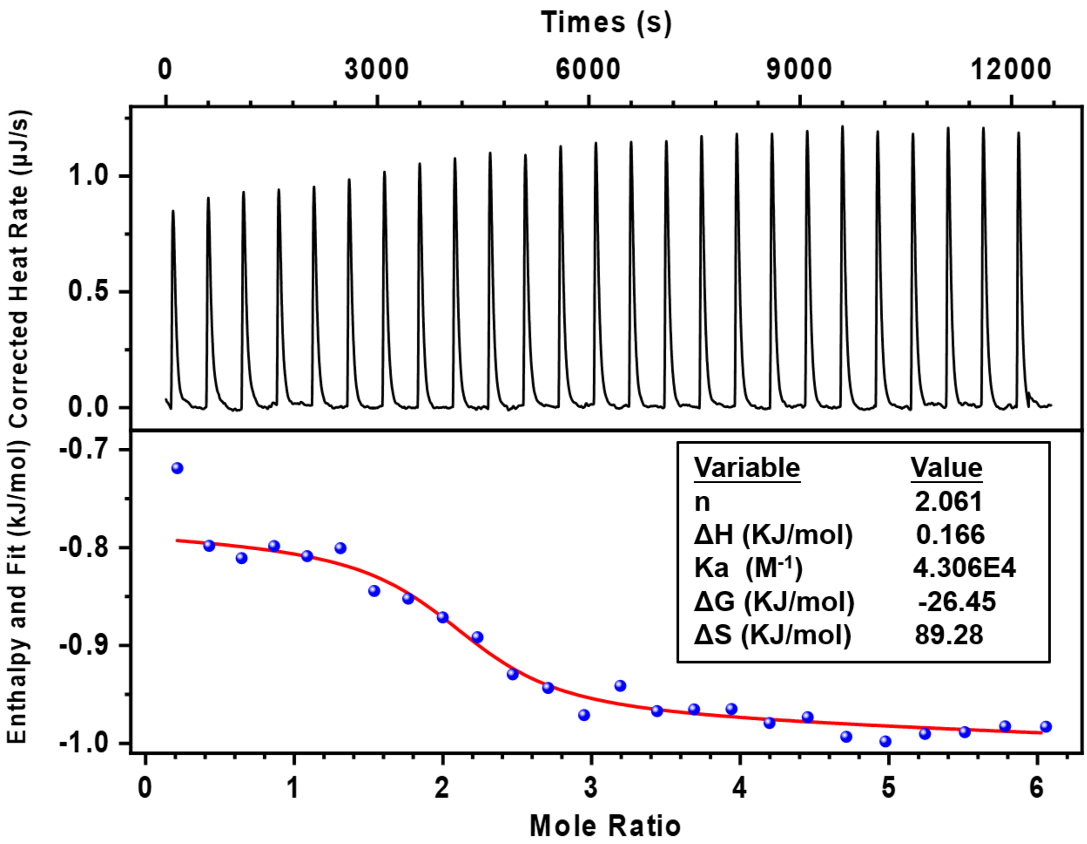

Figure S7. Microcalorimetric titration of Zn−**ZPD** with substrate **1** in CH_3CN/H_2O (4:1 in v:v, pH = 4.50) at 298.15 K. (top) Raw data for sequential 25 injections (10 µL per injection) of substrate **1** solution (2 mM) injecting into Zn−**ZPD** solution (0.10 mM). (bottom) Apparent reaction heat obtained from the integration of calorimetric traces.

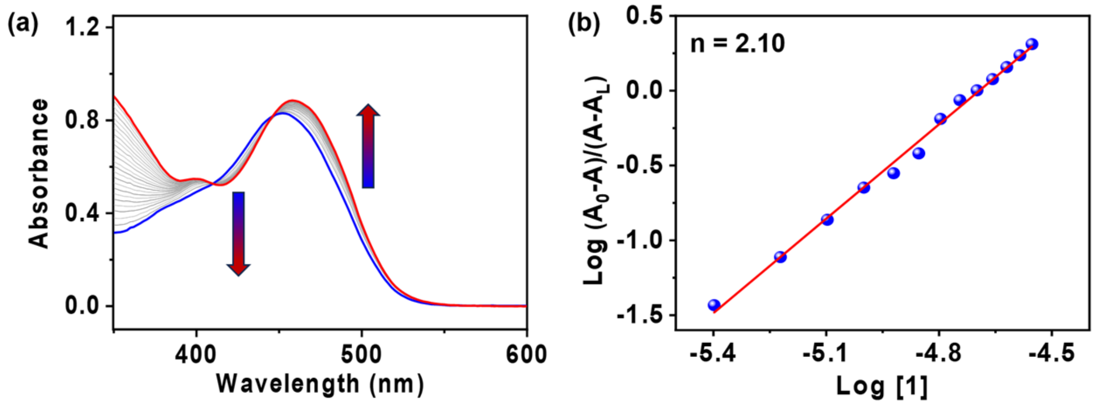

Figure S8. (a) Family of the UV-vis absorption spectra of Zn−**ZPD** (10 μM) upon addition of substrate **1** in CH_3CN/H_2O (4:1 in v:v, pH = 4.50); (b) Hill-plot linear fitting of the titration curve at 472 nm.

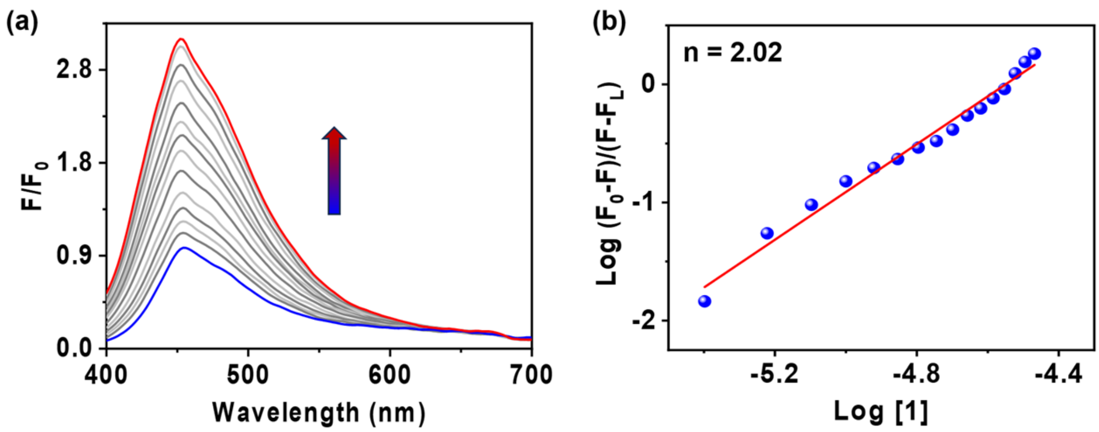

Figure S9. (a) Family of the luminescence spectra of Zn−**ZPD** (10 μM) upon addition of substrate **1** in CH_3CN/H_2O (4:1 in v:v, pH = 4.50); (b) Hill-plot linear fitting of the titration curve at 452 nm. Fluorescence intensity was excited at 380 nm.

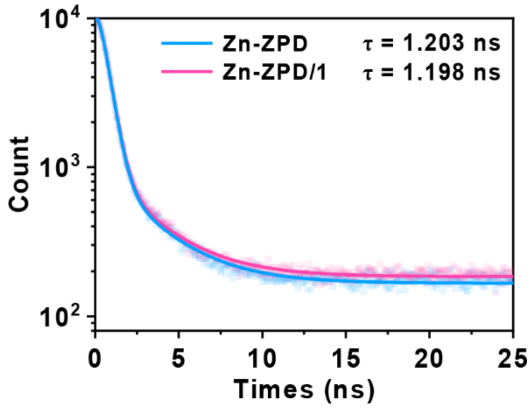

Figure S10. Luminescence decay of Zn−**ZPD** with or without substrate **1** in CH_3CN/H_2O.

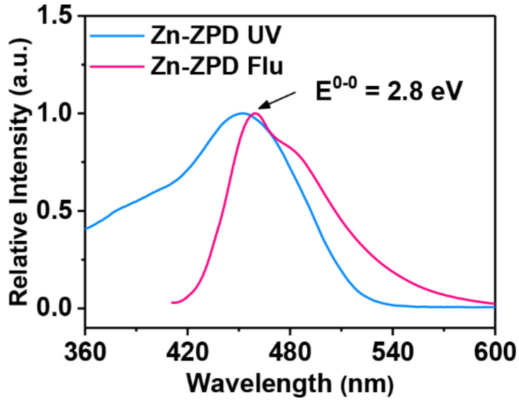

Figure S11. Normalized UV-Vis and luminescence spectra of Zn−**ZPD** showing the free energy change $E^{0\text{-}0}$.

5. Control experiments

5.1 ESI-MS for Zn−ZPB

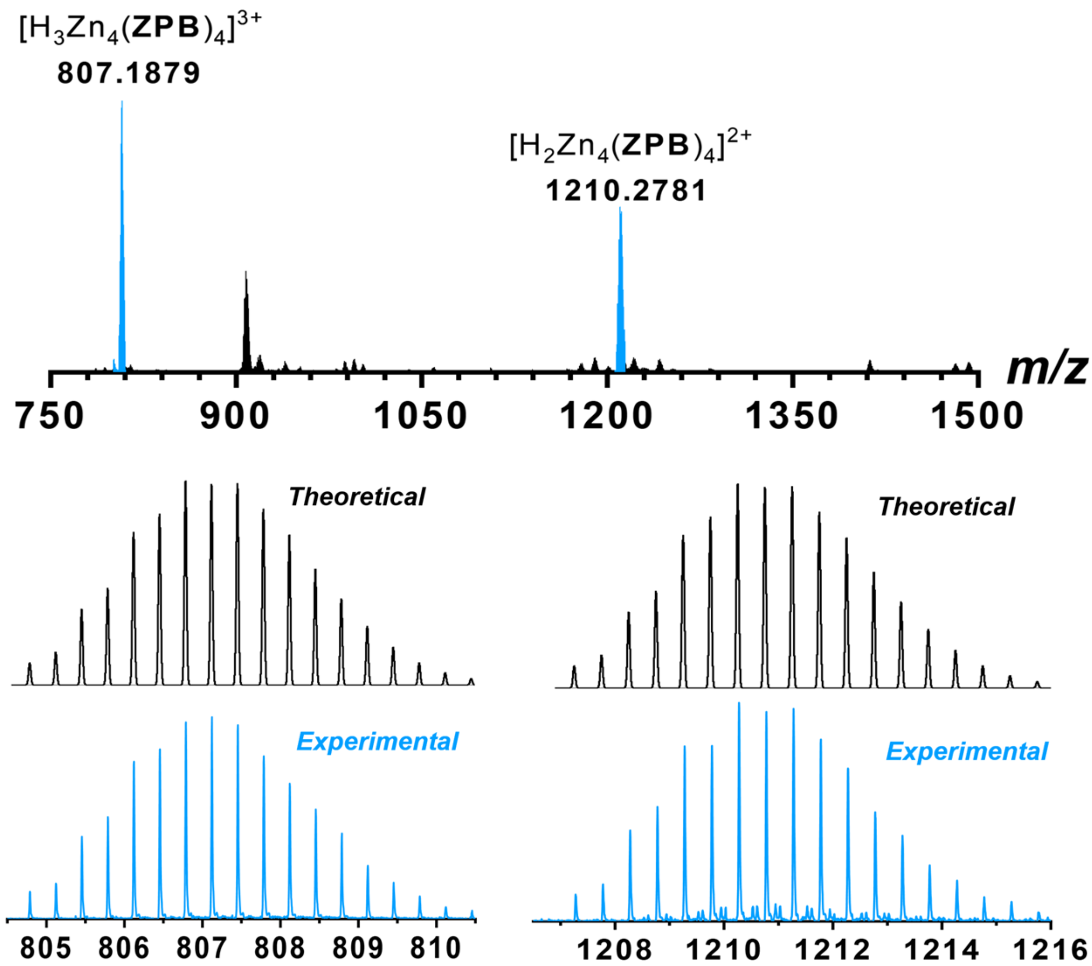

Peak	Value of *m/z*	Species assigned
1	807.1879	$[H_3Zn_4(\mathbf{ZPB})_4]^{3+}$
2	1210.2781	$[H_2Zn_4(\mathbf{ZPB})_4]^{2+}$

Figure S12. ESI-MS of Zn−**ZPB** (0.1 mM) in CH_3CN. The insets showed the theoretical and experimental isotopic patterns at *m/z* = 807.1879, and 1210.2781.

5.2 Inhibition Experiment

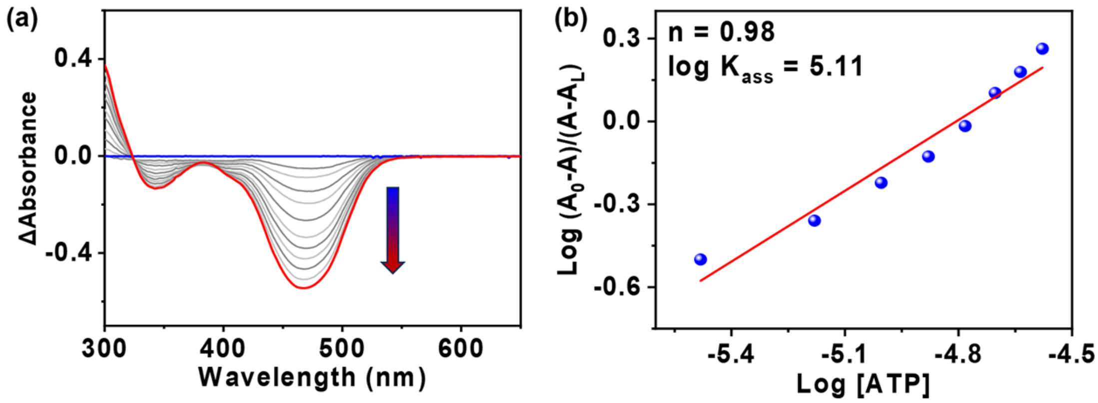

Figure S13. (a) Family of the UV-vis absorption difference spectra of Zn−**ZPD** (10 μM) upon addition of ATP in CH_3CN/H_2O (4:1 in v:v, pH = 4.50); (b) Hill-plot linear fitting at 462 nm.

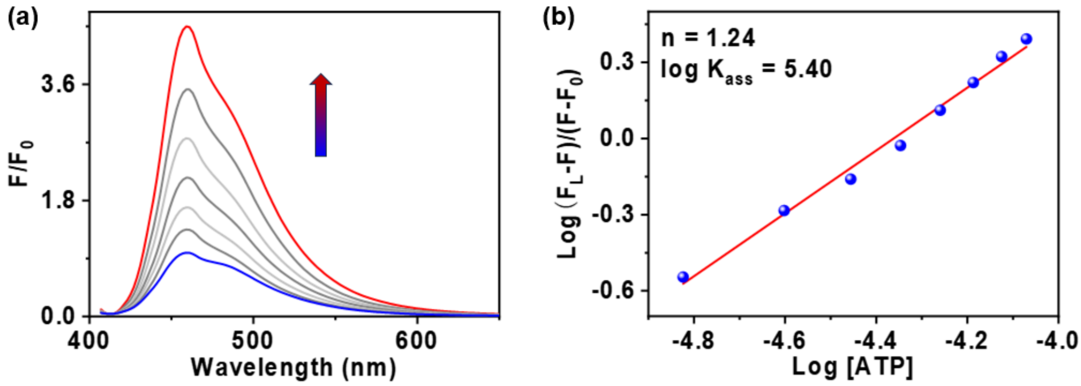

Figure S14 (a) Family of the luminescence spectra of Zn−**ZPD** (10 μM) upon addition of ATP in CH_3CN/H_2O (4:1 in v:v, pH = 4.50); (b) Hill-plot linear fitting at 452 nm. Fluorescence intensity was excited at 380 nm

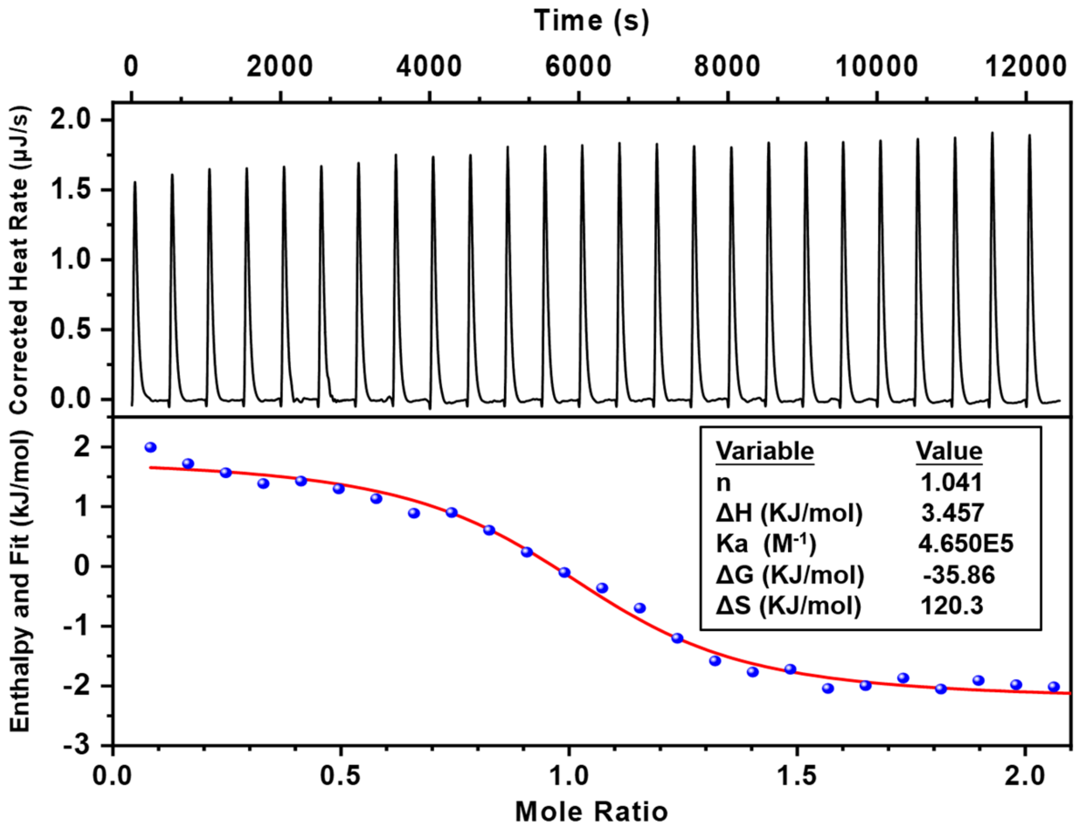

Figure S15. Microcalorimetric titration of Zn−**ZPD** with ATP in CH_3CN/H_2O (4:1 in v:v, pH = 4.50) at 298.15 K. (top) Raw data for sequential 25 injections (5 μL per injection) of ATP solution (2 mM) injecting into Zn−**ZPD** solution (0.10 mM). (bottom) Apparent reaction heat obtained from the integration of calorimetric traces.

6. Data Relative to Photocatalytic Hydrogenation

Standard conditions for hydrogenation of benzoxazinones

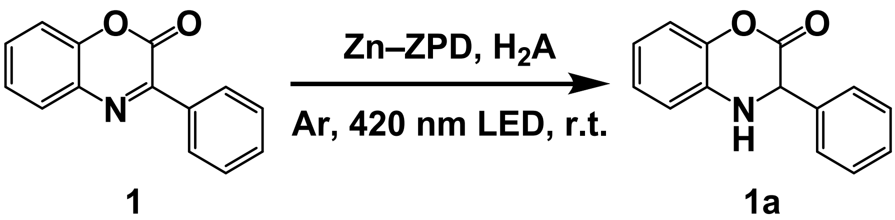

Zn−**ZPD** (40 μM), H_2A (0.1 mM) and substrate **1** (4.0 mM) was added in a 20 mL flask to obtain a total volume of 5.0 mL CH_3CN/H_2O (4:1 in v:v, pH = 4.50). The flask was sealed with a septum, degassed by bubbling argon for 15 min under atmospheric pressure at room temperature. After that, the samples were irradiated with a 420-nm-wavelength LED light for 12 hours, and the reaction temperature was kept at 298 K using a water filter.

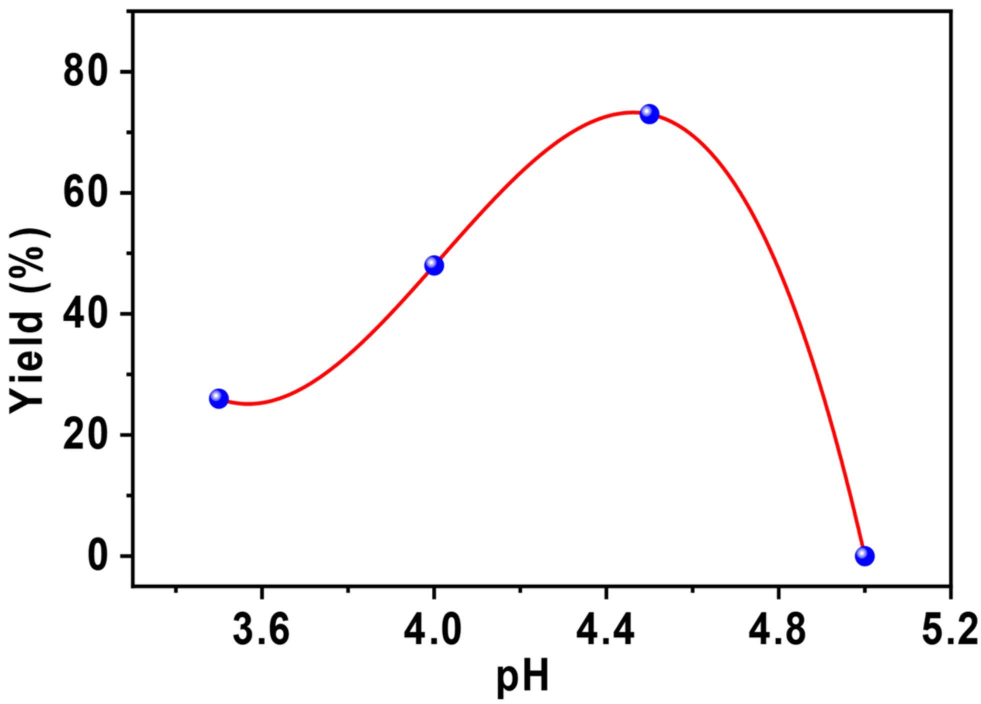

Figure S16. The yield of product **1a** at different pH in CH_3CN/H_2O (4:1 in v:v, pH = 4.50), the result indicated that the optimal pH was at 4.5.

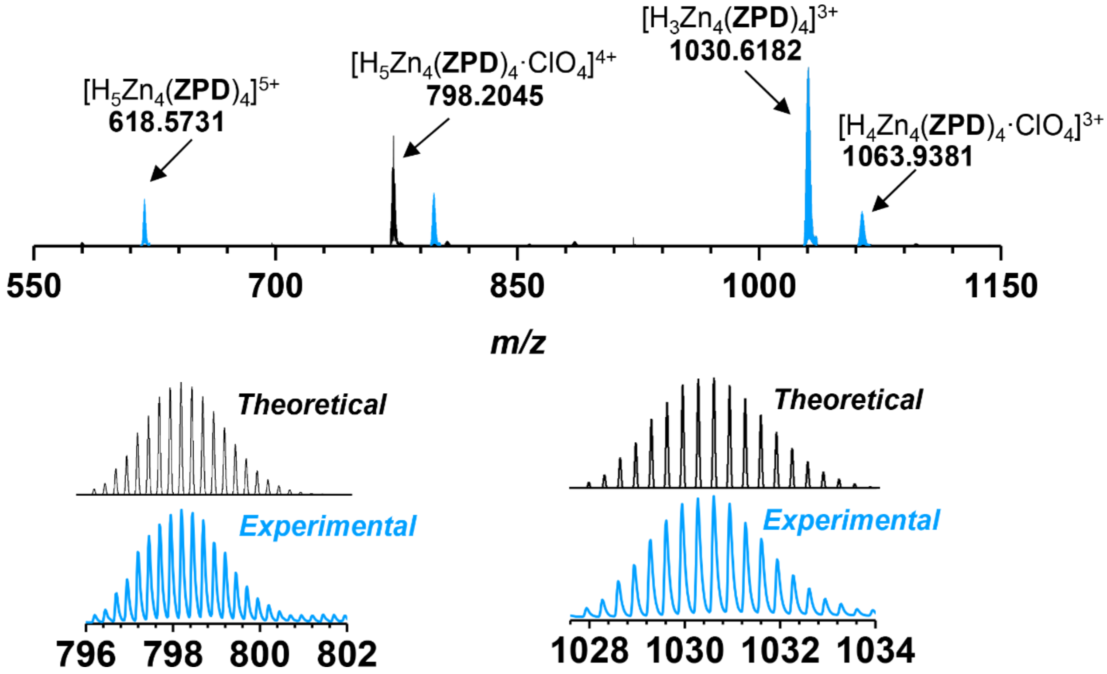

Figure S17. ESI-MS of Zn−**ZPD** after reaction under standard catalytic conditions. The inserts showed the theoretical and experimental isotopic patterns at *m/z* = 798.2045 and 1030.6182.

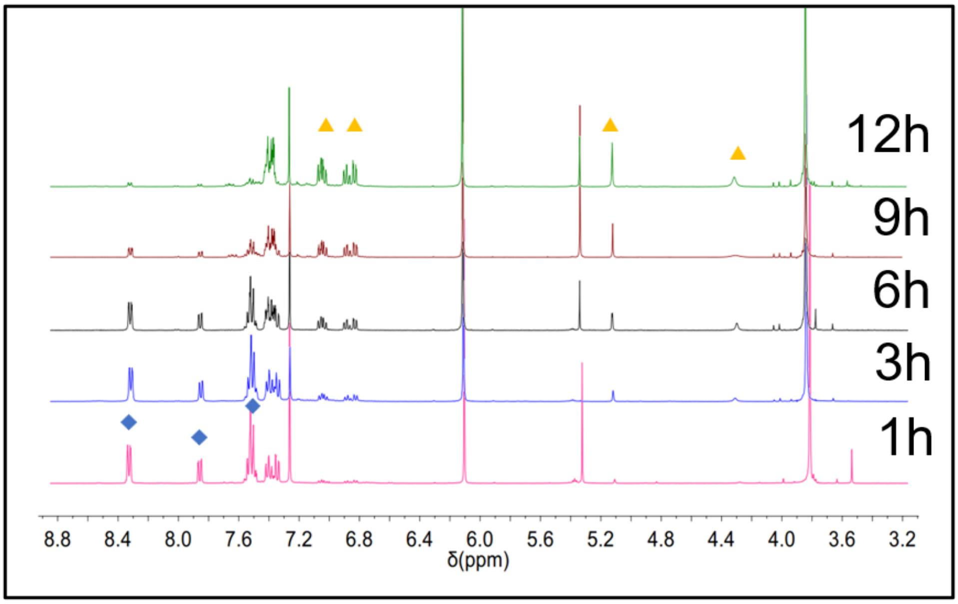

Figure S18 ^{1}H NMR ($CDCl_3$, 400 MHz) monitoring of the biomimetic hydrogenation progress using Zn−**ZPD**, showing the increasing tendency of the peaks on the products (yellow triangles), while the gradual vanishes of the peaks on the substrate **1** (blue rhombuses) with the proceeding of the reaction. The peaks are internal standard at around 6.10 (1,3,5-trimethoxybenzen).

7. Additional NMR Spectra

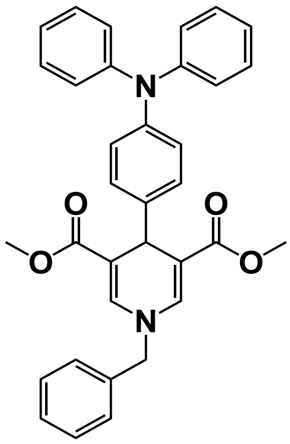

Dimethyl 1-benzyl-4-phenyl-1,4-dihydropyridine-3,5-dicarboxylate:

^{1}H NMR (400 MHz, DMSO-d_6, *ppm*): δ 7.50 (s, 2H), 7.41-7.37 (m, 2H), 7.35-7.33 (m, 2H), 7.30-7.26 (m, 5H), 7.05-6.99 (m, 4H), 6.96-6.93 (m, 4H), 6.82-6.80 (m, 2H), 4.80 (s, 2H), 4.69 (s, 1H), 3.58 (s, 6H).

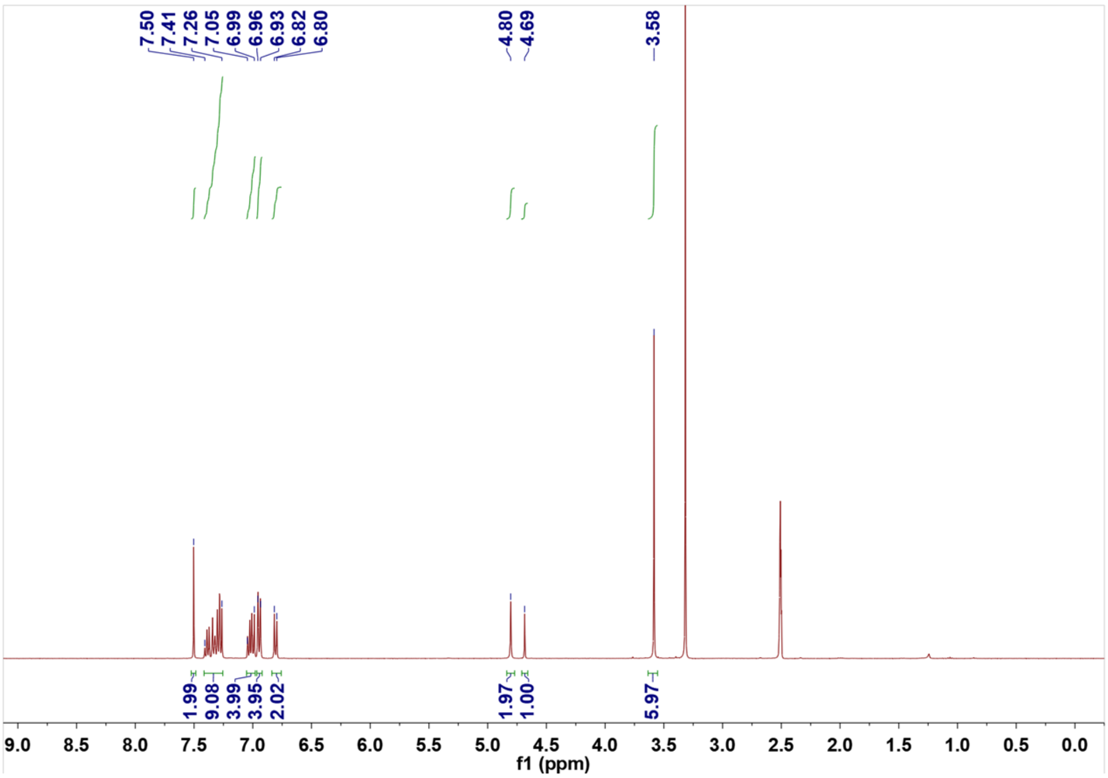

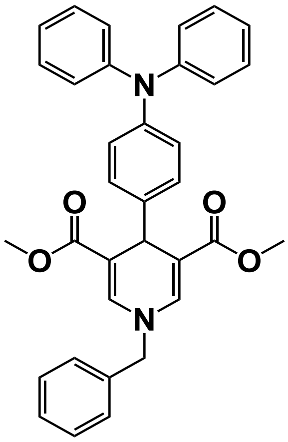

Dimethyl 1-benzyl-4-phenyl-1,4-dihydropyridine-3,5-dicarboxylate:

^{13}C NMR (101 MHz, DMSO-d_6, *ppm*): δ 191.04, 166.64, 147.60, 135.07, 131.46, 130.51, 129.97, 126.88, 124.75, 124.43, 123.61, 123.26, 120.29, 118.64, 117.33, 111.12, 51.97, 36.69.

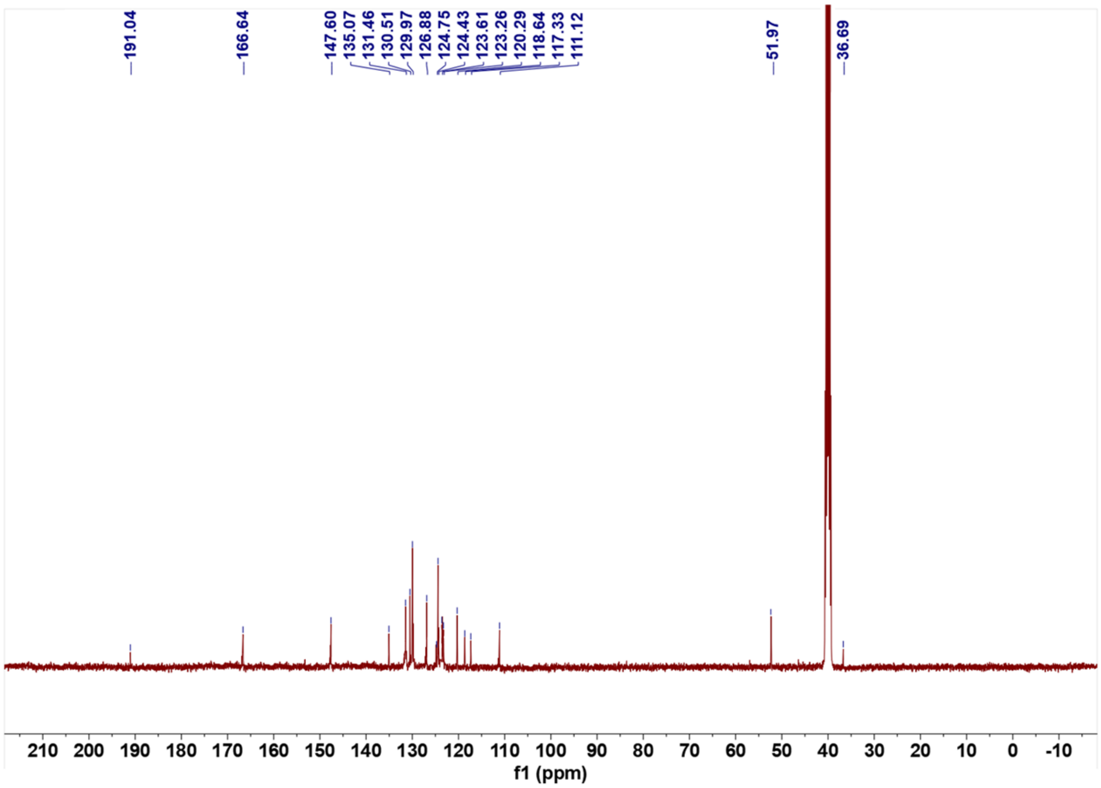

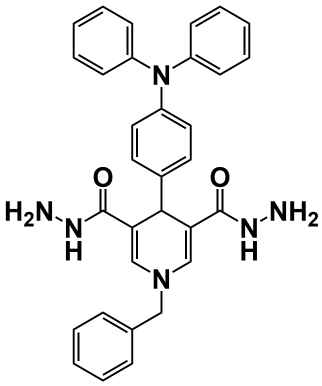

1-benzyl-4-(4-(diphenylamino)-phenyl)-1,4-dihydropyridine-3,5-dicarbohydra-zide:

^{1}H NMR (400 MHz, DMSO-d_6, *ppm*): δ 8.70 (s, 2H), 7.38-7.25 (m, 9H), 7.21 (s, 2H), 7.08-7.06 (m, 2H), 7.02-6.99 (m, 2H), 6.94-6.92 (m, 4H), 6.80-6.77 (m, 2H), 4.96 (s,1H), 4.59 (s, 2H), 4.15 (s, 4H).

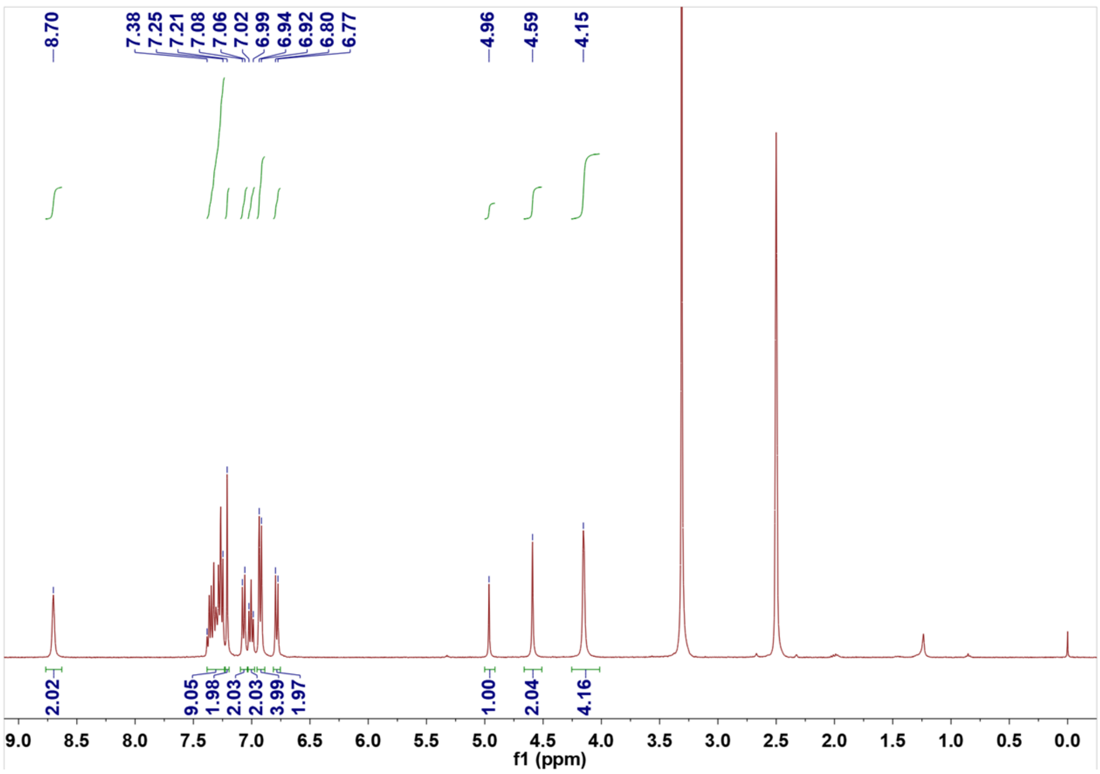

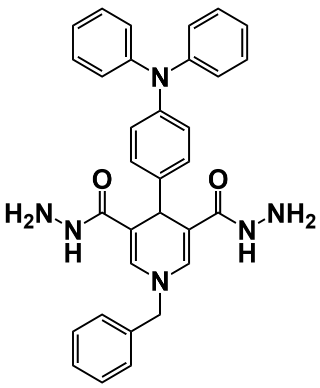

1-benzyl-4-(4-(diphenylamino)-phenyl)-1,4-dihydropyridine-3,5-dicarbohydra-zide:

^{13}C NMR (101 MHz, DMSO-d_6, *ppm*): 166.62, 147.25, 145.07, 141.18, 137.81, 133.83, 129.41, 128.64, 128.46, 127.65, 127.54, 123.49, 123.29, 122.67, 108.39, 56.85, 34.48.

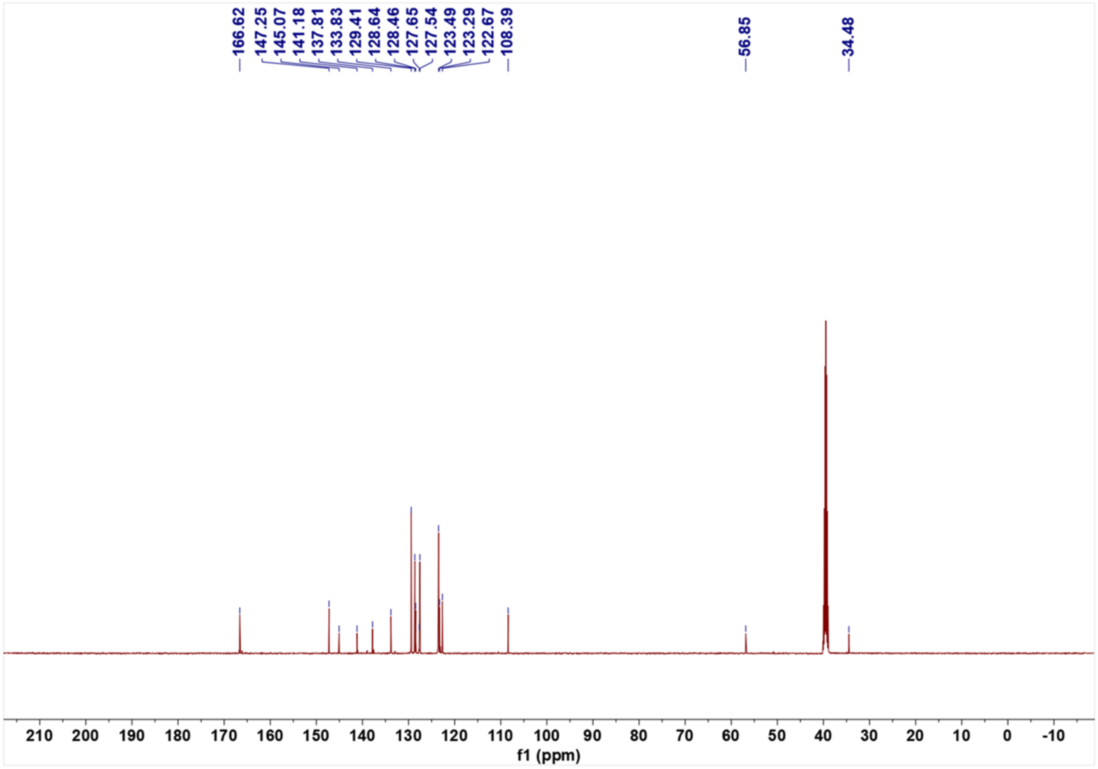

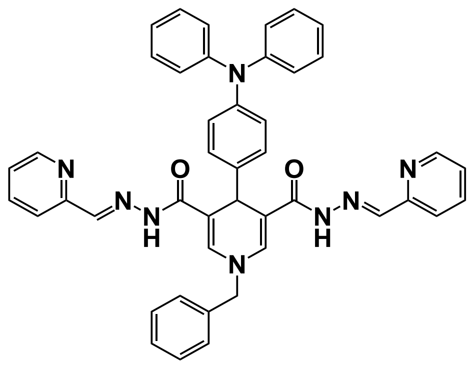

H_2**ZPD**: [1]H NMR (400 MHz, DMSO-d_6, *ppm*): δ 11.41 (s, 2H), 8.59-8.58 (d, *J* = 4.8 Hz, 2H), 8.25 (s, 2H), 7.84 (m, 4H), 7.53 (s, 2H), 7.43-7.32 (m, 7H),7.26-7.23 (m, 4H), 7.18-7.16 (m, 2H), 7.00-6.97 (m, 2H), 6.94-6.92 (m, 4H), 6.86-6.84 (m, 2H), 5.30 (s, 1H), 4.77 (s, 2H).

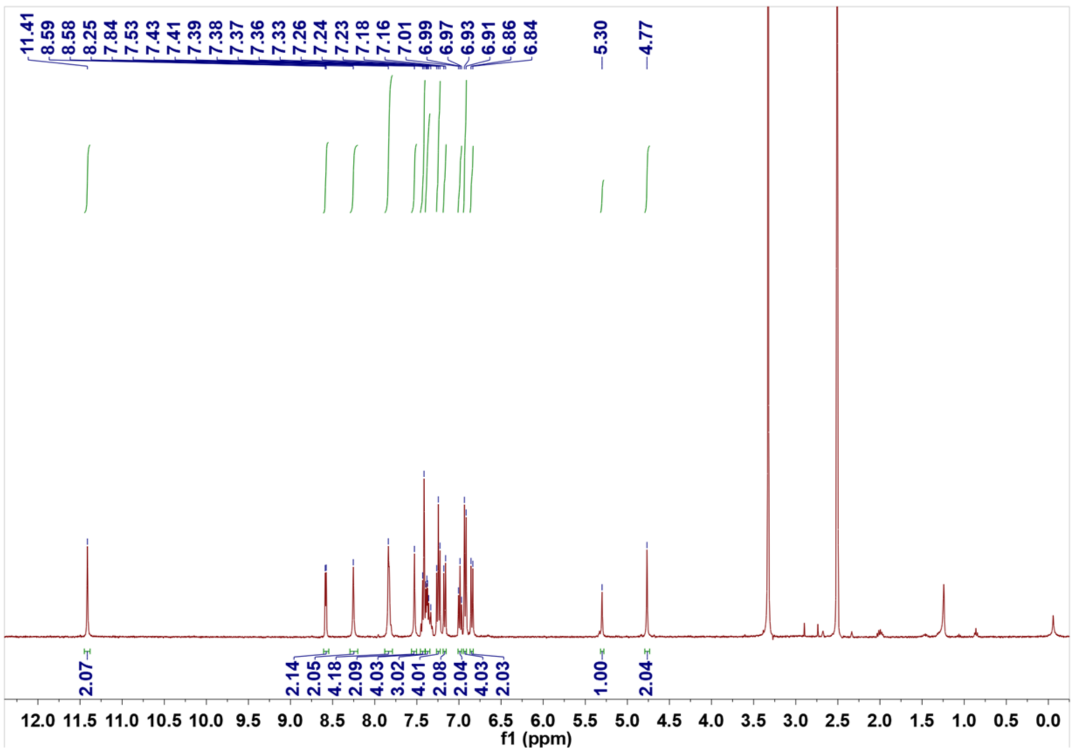

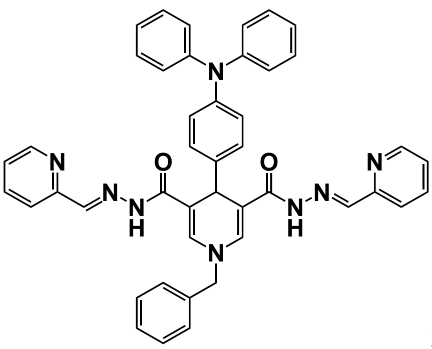

23

H_2**ZPD**: [13]C NMR (101 MHz, DMSO-d_6, *ppm*) δ: 164.42, 153.99, 149.90, 147.71, 145.82, 145.72, 141.59, 138.16, 137.18, 136.13, 129.92, 129.08, 128.28, 127.74, 124.46, 124.10, 123.71, 123.22, 120.03, 109.40, 57.66, 35.69.

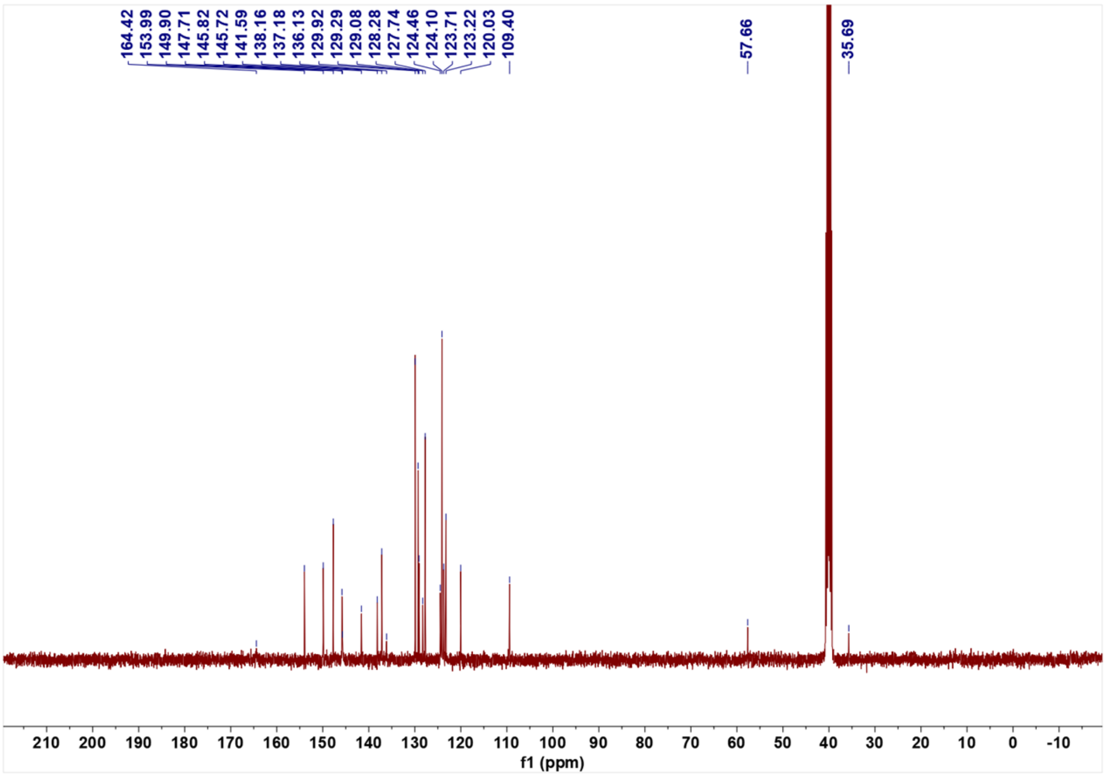

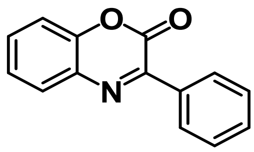

3-phenyl-*2H*-1,4-benzoxazin-2-one: [1]H NMR (400 MHz, $CDCl_3$, *ppm*): δ 8.33 (d, *J* = 7.2 Hz, 2H), 7.86 (d, *J* = 8.0 Hz, 1H), 7.56-7.49 (m, 4H), 7.40 (t, *J* = 7.6 Hz, 1H), 7.34 (d, *J* = 8.0 Hz, 1H).

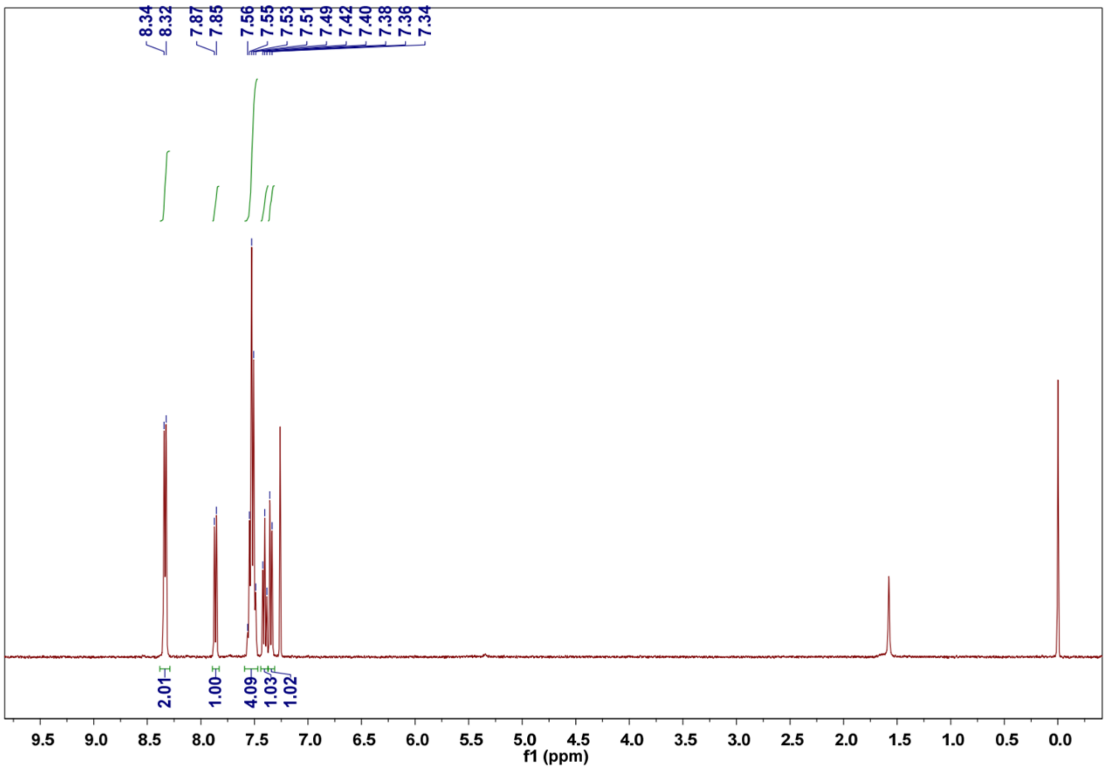

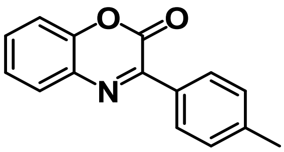

3-(4-tolyl)-*2H*-1,4-benzoxazin-2-one: [1]H NMR (400 MHz, $CDCl_3$, *ppm*): δ 8.26 (d, *J* = 7.6 Hz, 2H), 7.84 (d, *J* = 8.0 Hz, 1H), 7.50 (t, *J* = 8.0 Hz, 1H), 7.38 (t, *J* = 7.6 Hz, 1H), 7.31 (t, *J* = 7.6 Hz, 3H), 2.44 (s, 3H).

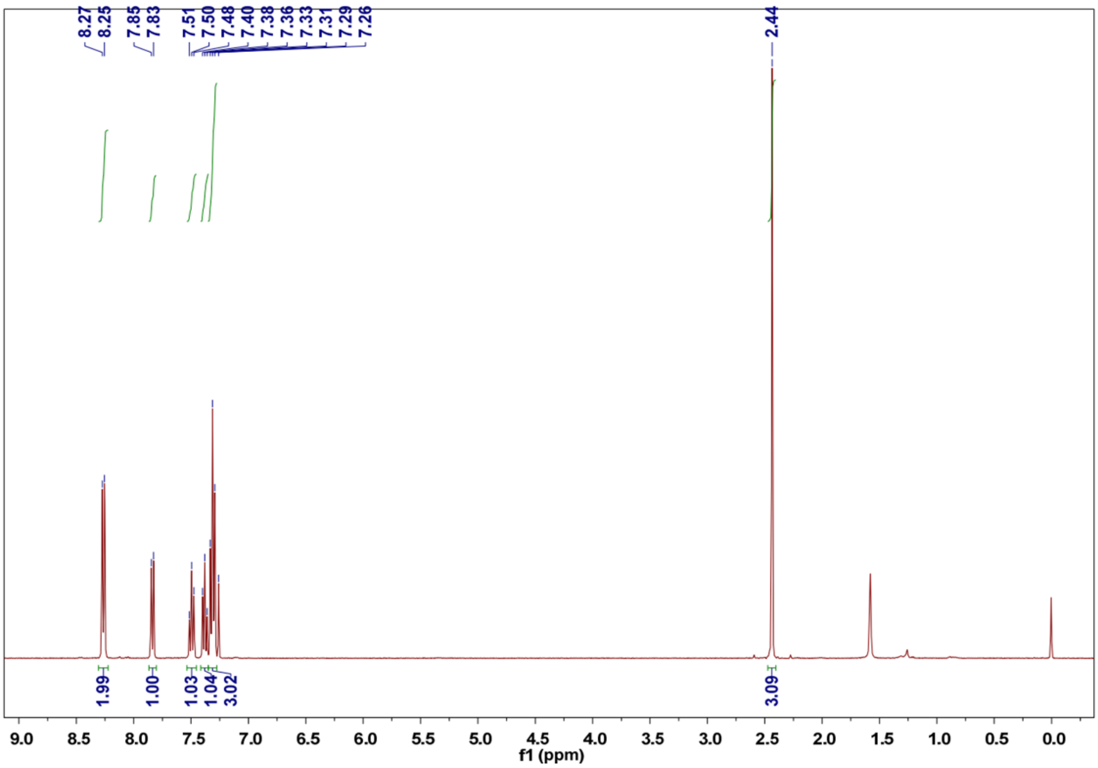

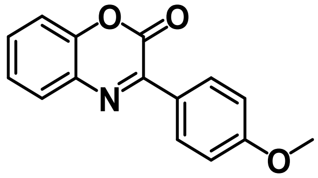

3-(4-methoxyphenyl)-*2H*-1,4-benzoxazin-2-one: ^{1}H NMR (400 MHz, $CDCl_3$, *ppm*): δ 8.42–8.38 (m, 2H), 7.82 (dd, *J* = 8.0, 1.6 Hz, 1H), 7.48 (td, *J* = 7.6, 1.6 Hz, 1H), 7.39-7.30 (m, 2H), 7.01 (dt, *J* = 8.8, 3.2 Hz, 2H), 3.89 (s, 3H).

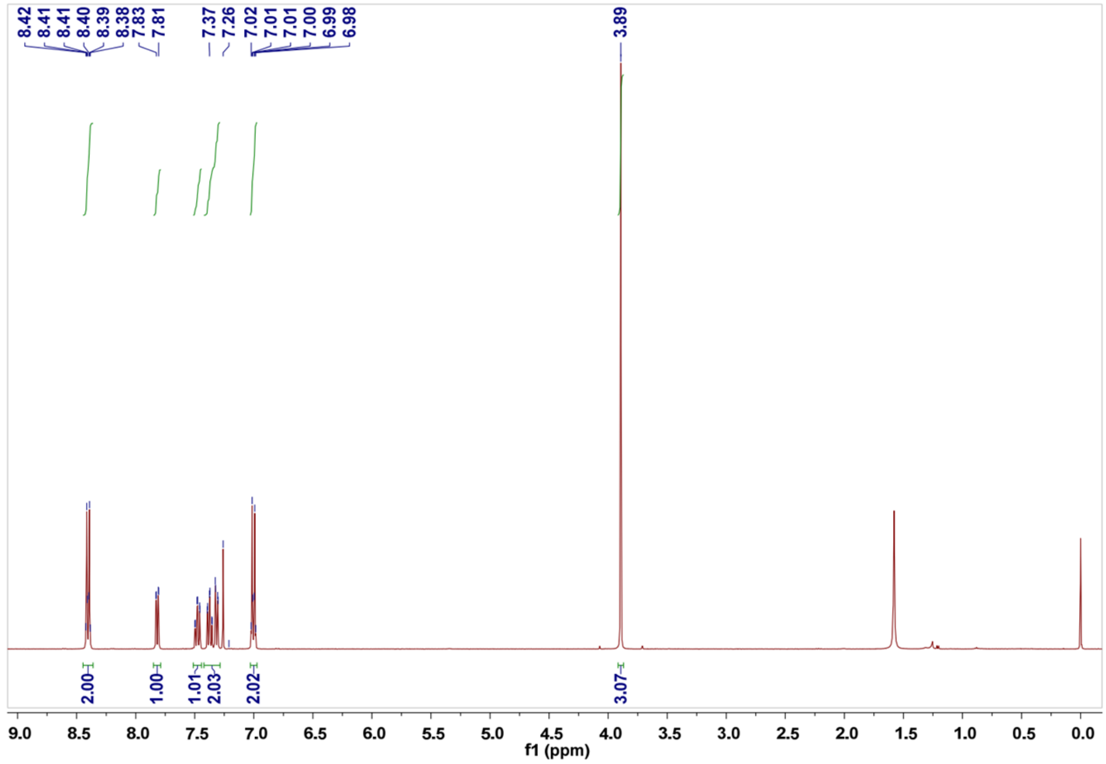

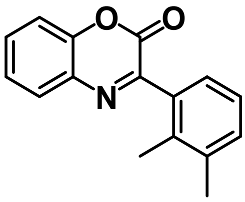

3-(2, 3-dimethyphenyl)-*2H*-1,4-benzoxazin-2-one: ^{1}H NMR (400 MHz, $CDCl_3$, *ppm*): δ 8.11-8.09 (m, 2H), 7.84 (d, *J* = 7.6 Hz, 1H), 7.52-7.48 (m, 1H), 7.40-7.31 (m, 2H), 7.26-7.25 (m, 1H), 2.36-2.34 (m, 6H).

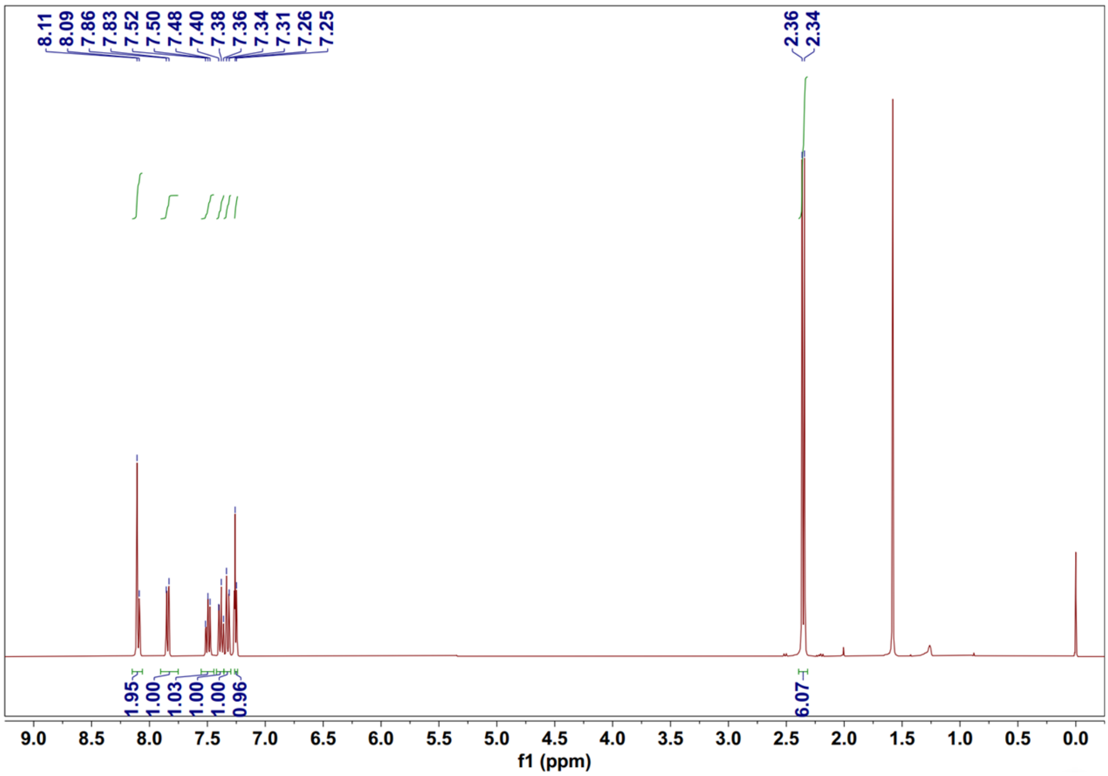

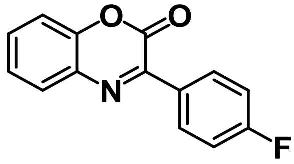

3-(4-fluorophenyl)-*2H*-1,4-benzoxazin-2-one: ^{1}H NMR (400 MHz, $CDCl_3$, *ppm*): δ 8.43-8.40 (m, 2H), 7.84 (dd, *J* = 7.6 Hz, 1.2 Hz, 1H), 7.55-7.51 (m, 1H), 7.42-7.33 (m, 2H), 7.20-7.16 (m, 2H).

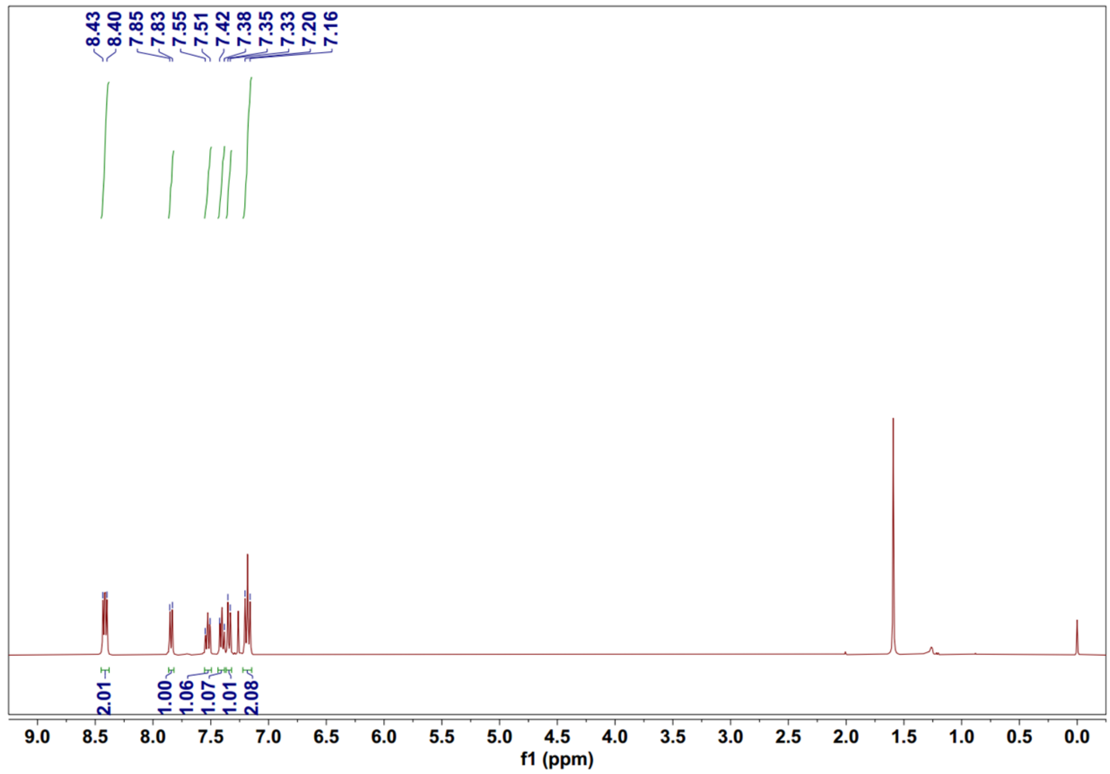

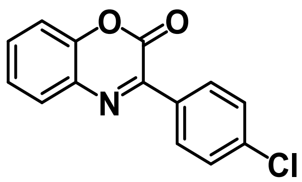

3-(4-chlorophenyl)-*2H*-1,4-benzoxazin-2-one: ^{1}H NMR (400 MHz, $CDCl_3$, *ppm*): δ 8.36-8.34 (m, 2H), 7.84 (dd, *J* = 7.2, 1.6 Hz, 1H), 7.56-7.52 (m, 1H), 7.48-7.46 (m, 2H), 7.43-7.39 (m, 1H), 7.34 (dd, *J* = 8.0, 1.2 Hz, 1H);

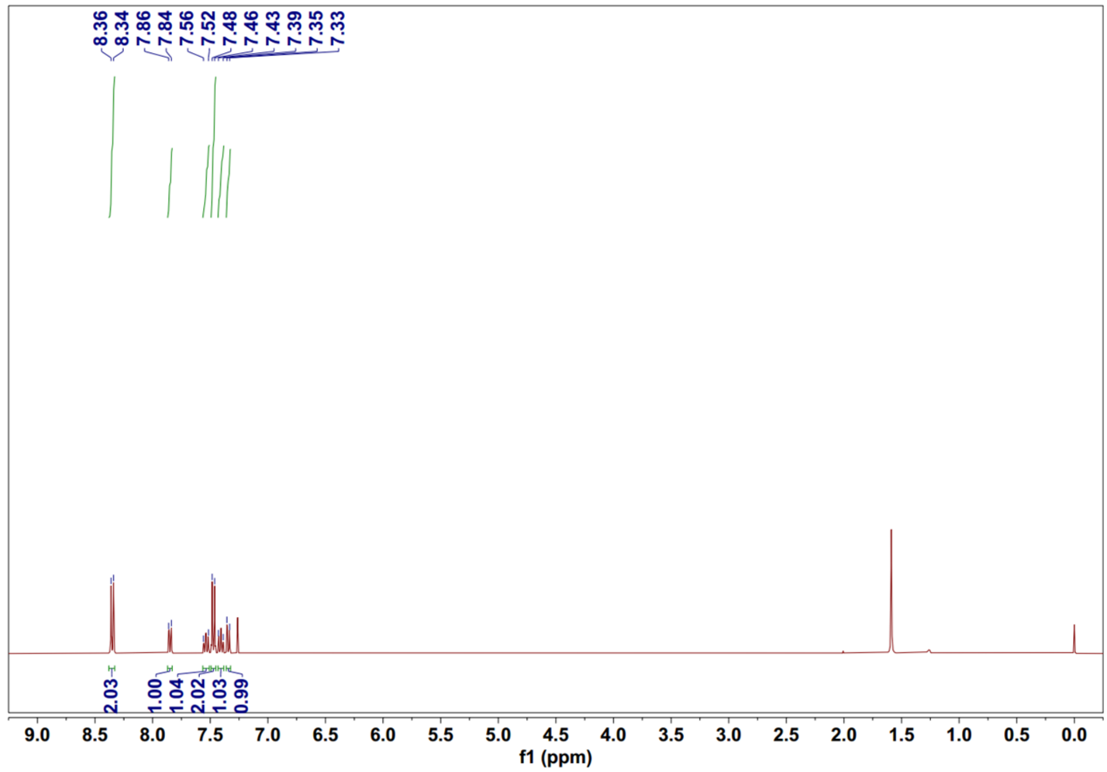

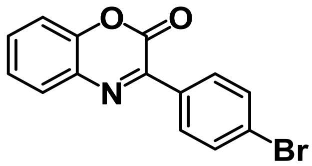

3-(4-bromophenyl)-*2H*-1,4-benzoxazin-2-one: [1]H NMR (400 MHz, $CDCl_3$, *ppm*): δ 8.28-8.26 (m, 2H), 7.85 (dd, *J* = 8.4, 1.6 Hz, 1H), 7.65-7.62 (m 2H), 7.56-7.52 (m, 1H), 7.43-7.39 (m, 1H), 7.34 (dd, *J* = 8.4, 1.2 Hz, 1H).

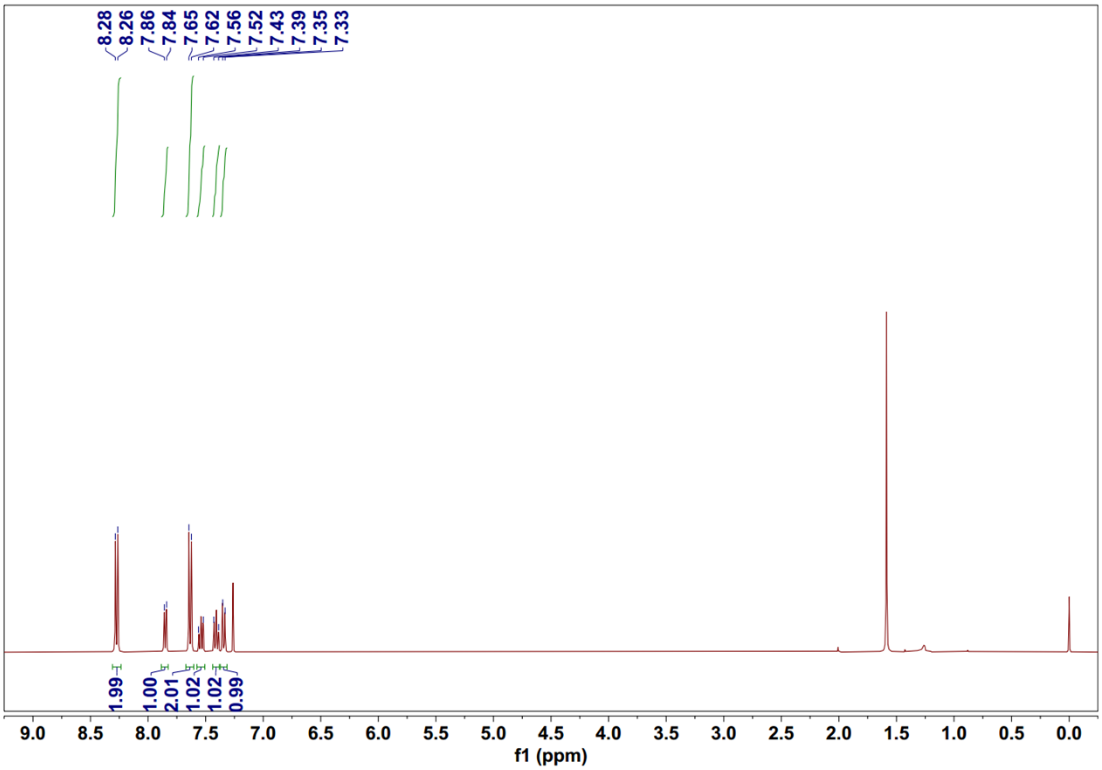

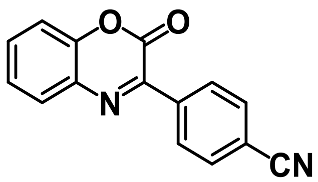

3-(4-nitrilephenyl)-*2H*-1,4-benzoxazin-2-one: ^{1}H NMR (400 MHz, $CDCl_3$, *ppm*): δ 8.52 (d, *J* = 7.6 Hz, 2H), 7.89 (d, *J* = 8.0 Hz, 1H), 7.80 (d, *J* = 8.8 Hz, 2H), 7.62-7.57 (m, 1H), 7.45 (t, *J* = 7.6 Hz, 1H), 7.38 (d, *J* = 8.4 Hz, 1H).

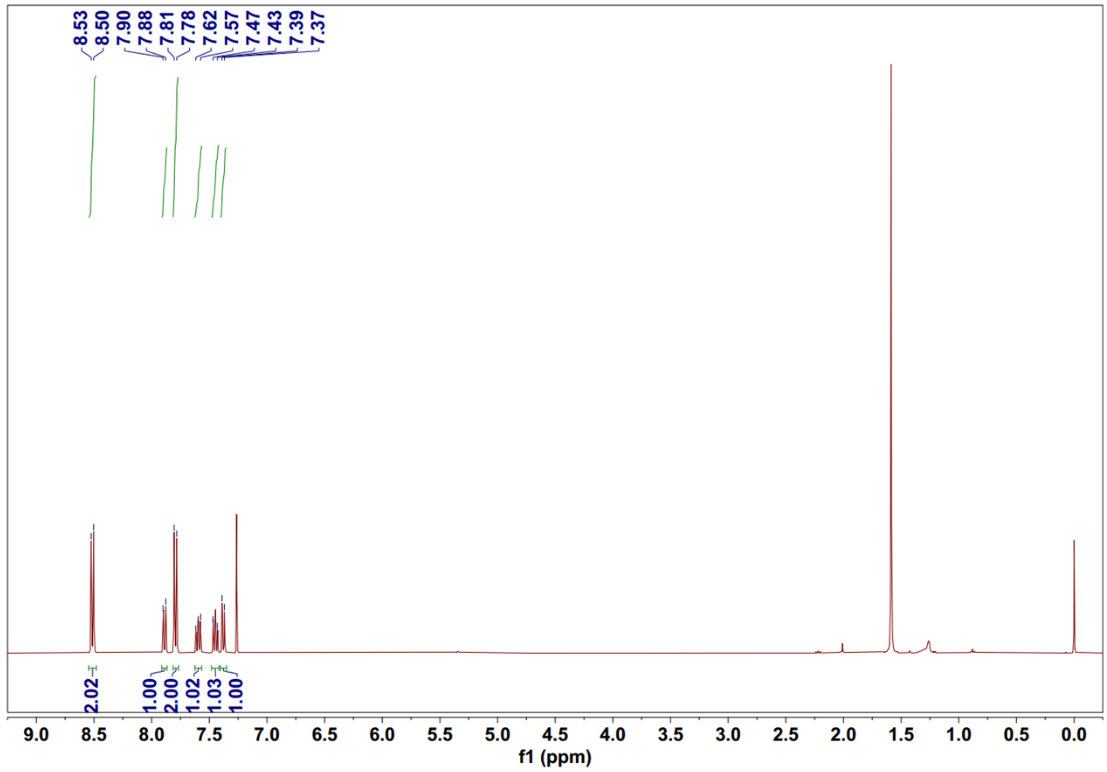

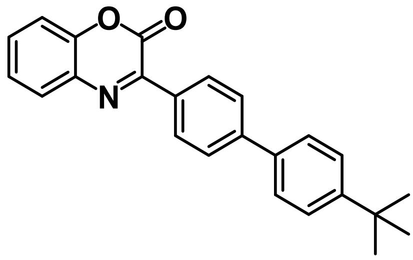

3-(4'-(*tert*-butyl)-[1,1'-biphenyl]-4-yl)-*2H*-1,4-benzoxazin-2-one: [1]H NMR (400 MHz, $CDCl_3$, *ppm*): δ 8.45 (dt, *J* = 8.8, 2.0 Hz, 2H), 7.87 (dd, *J* = 8.0, 1.2 Hz, 1H), 7.74 (dt, *J* = 8.4, 1.6 H, 2H), 7.62 (dt, *J* = 8.4, 2.0 Hz 2H), 7.55-7.50 (m, 3H), 7.41 (td, *J* = 7.6, 1.2 Hz, 1H), 7.35 (dd, *J* = 8.0, 1.2 Hz, 1H), 1.38 (s, 9H).

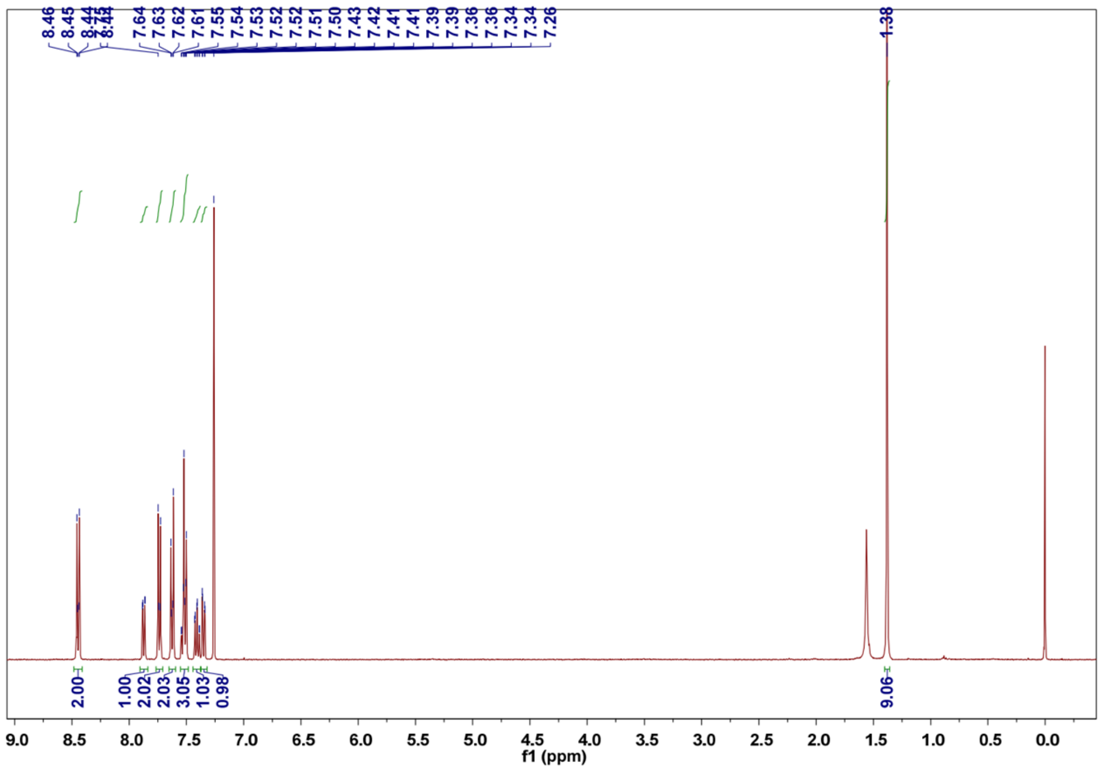

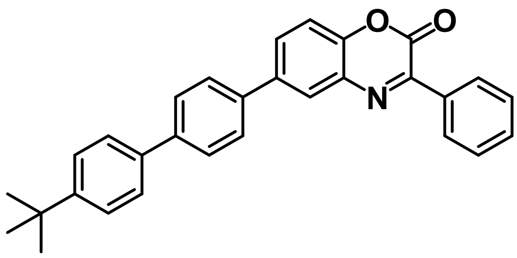

6-(4-(*tert*-butyl)phenyl)-3-phenyl-2H-1,4-benzoxazin-2-one: ^{1}H NMR (400 MHz, $CDCl_3$, *ppm*): δ 8.36 (dd, *J* = 7.6, 1.2 Hz, 2H), 8.08 (d, *J* = 2.0 Hz, 1H), 7.75 (dd, *J* = 8.8, 2.4 Hz, 1H), 7.61-7.59 (m, 2H), 7.55–7.49 (m, 5H), 7.39 (d, *J* = 8.4 Hz, 1H), 1.39 (s, 9H).

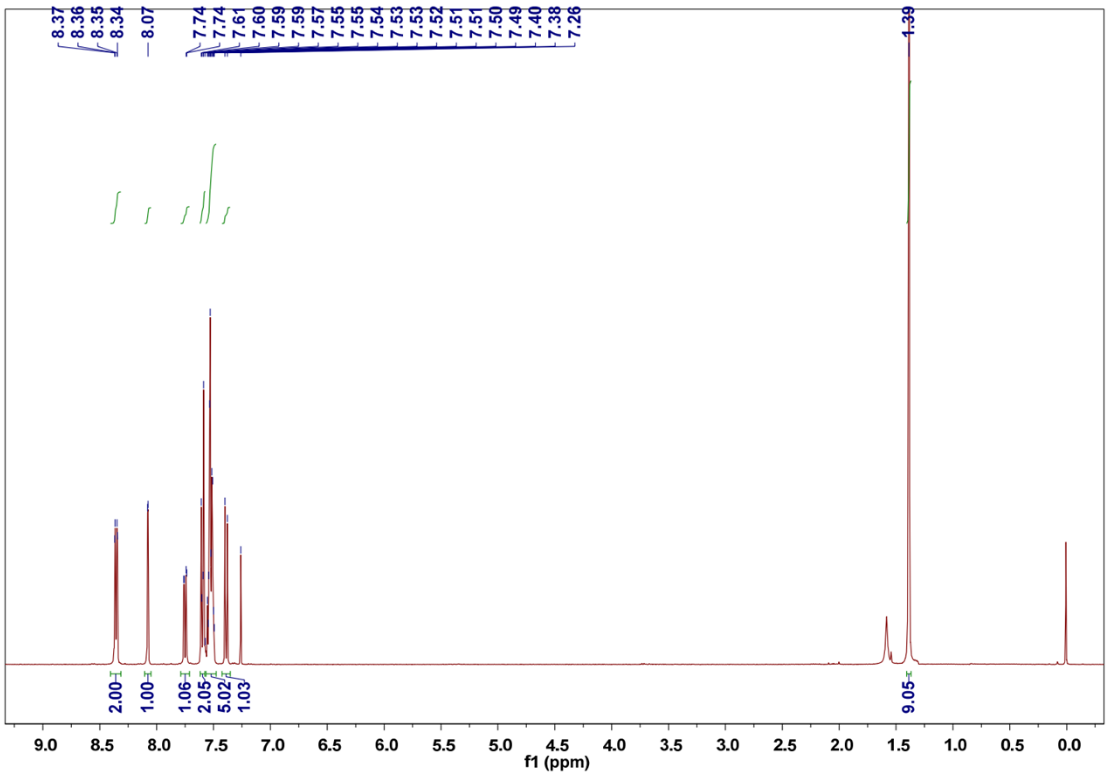

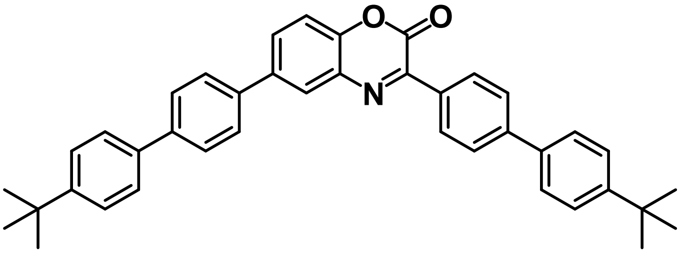

3-(4'-(*tert*-butyl)-[1,1'-biphenyl]-4-yl)-6-(4-(*tert*-butyl)phenyl)-*2H*-1,4-benzoxazin-2-one: ^{1}H NMR (400 MHz , $CDCl_3$, *ppm*): δ 8.33 (d, *J* = 8.0 Hz, 2H), 7.98 (s, 1H), 7.78 (d, *J* = 8.0 Hz, 2H), 7.64-7.59 (m, 6H), 7.53-7.51 (m, 4H). 1.39 (s, 18H).

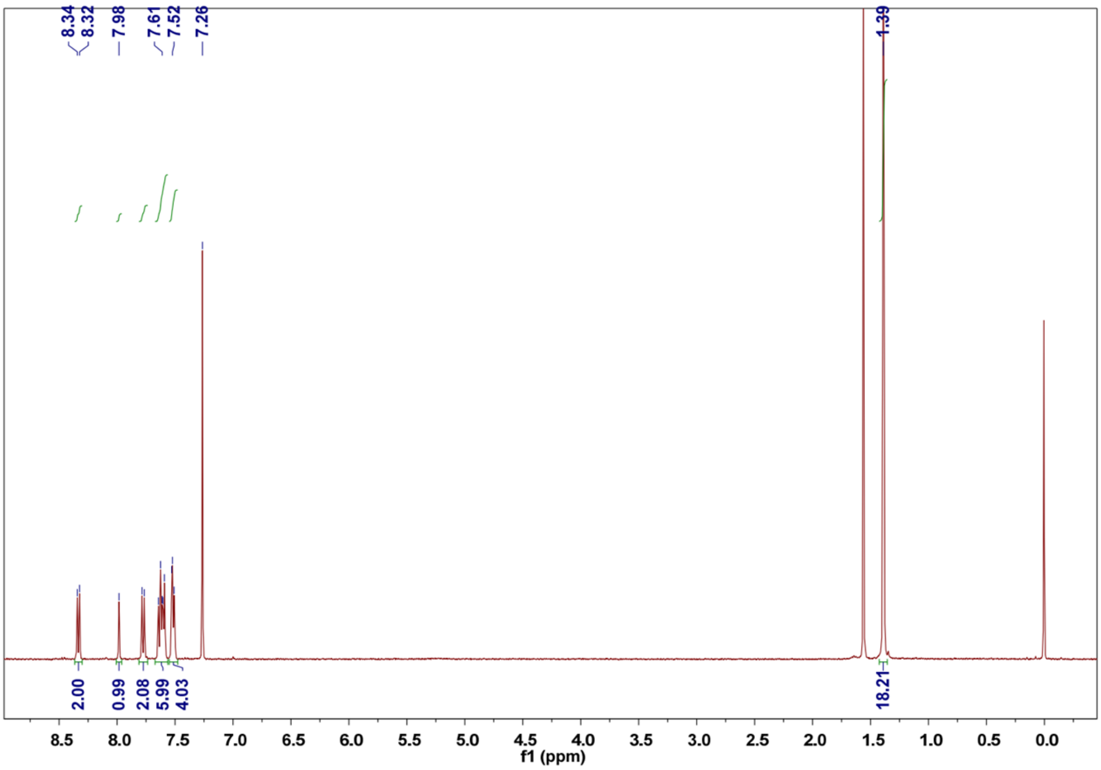

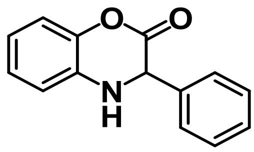

3-phenyl-3,4-dihydro-*2H*-benzo-1,4-oxazin-2-one: ^{1}H NMR (400 MHz, $CDCl_3$, *ppm*): δ 7.43-7.35 (m, 5H), 7.06-7.01 (m, 2H), 6.87 (td, *J* = 7.2, 1.6 Hz, 1H), 6.82 (dd, *J* = 7.6, 1.6 Hz, 1H), 5.07 (s, 1H), 4.26 (s, 1H).

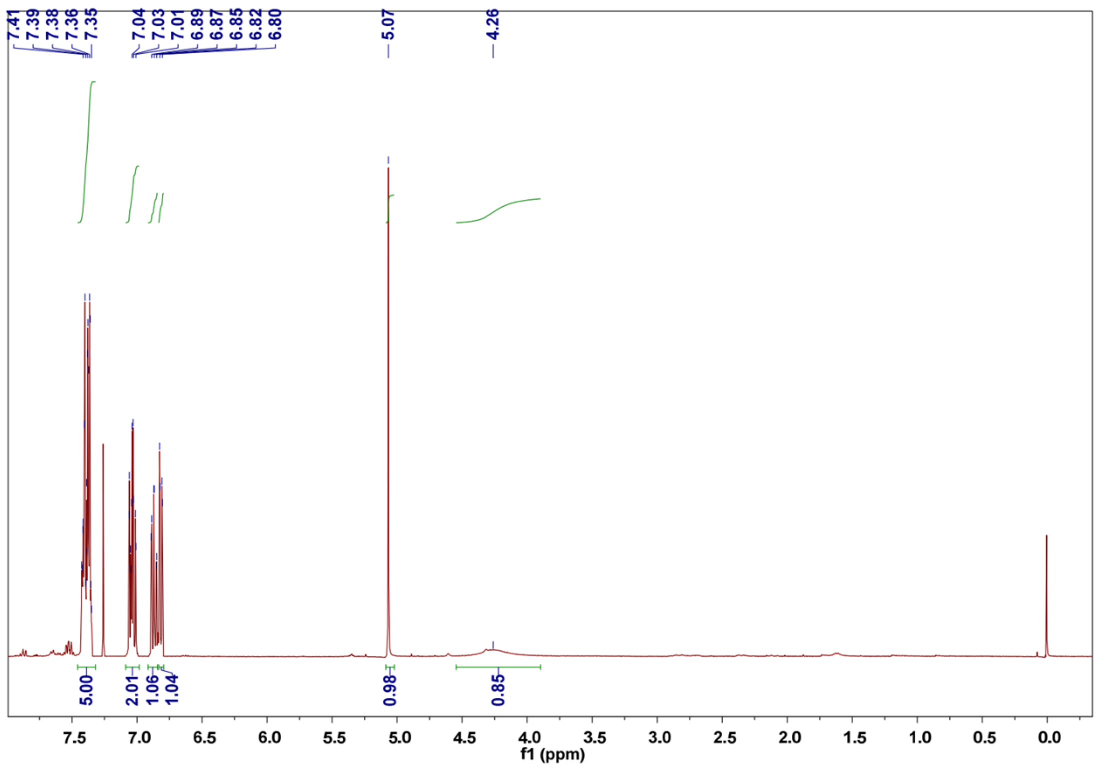

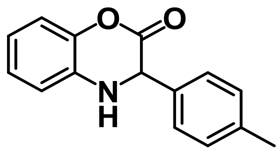

3-(4-tolyl)-3,4-dihydro-*2H*-benzo-1,4-oxazin-2-one: [1]H NMR (400 MHz, $CDCl_3$, *ppm*): δ 7.29 (d, *J* = 7.6 Hz, 2H), 7.18 (d, *J* = 7.6 Hz, 2H), 7.06-7.00 (m , 2H), 6.86 (t, *J* = 8.0 Hz, 1H), 6.80 (d, *J* = 7.6 Hz, 1H), 5.03 (s, 1H), 4.21 (s, 1H), 2.34 (s, 3H).

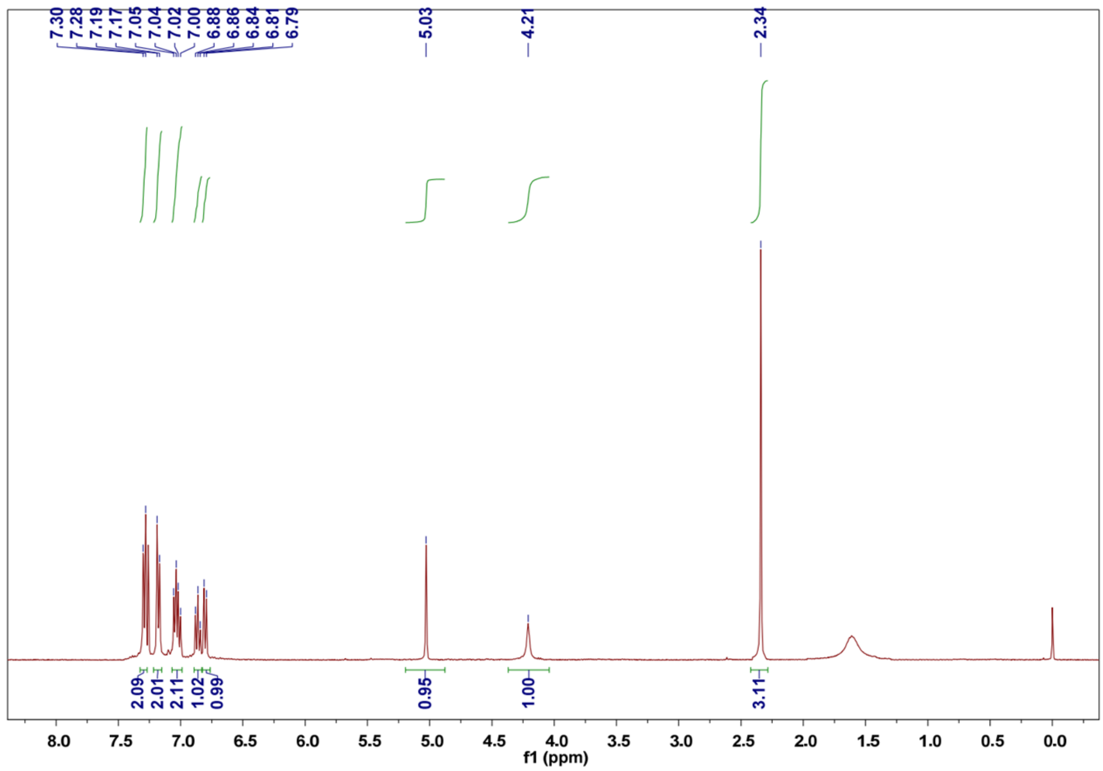

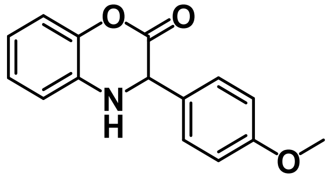

3-(4-methoxyphenyl)-3,4-dihydro-*2H*-benzo-1,4-oxazin-2-one: [1]H NMR (400 MHz, $CDCl_3$, *ppm*): δ 7.33 (d, *J* = 8.8 Hz, 2H), 7.07-7.00 (m, 2H), 6.91-6.89 (m, 3H), 6.80 (dd, *J* = 8.0, 1.6 Hz, 1H), 5.01 (s, 1H), 4.18 (s, 1H), 3.80 (s, 3H).

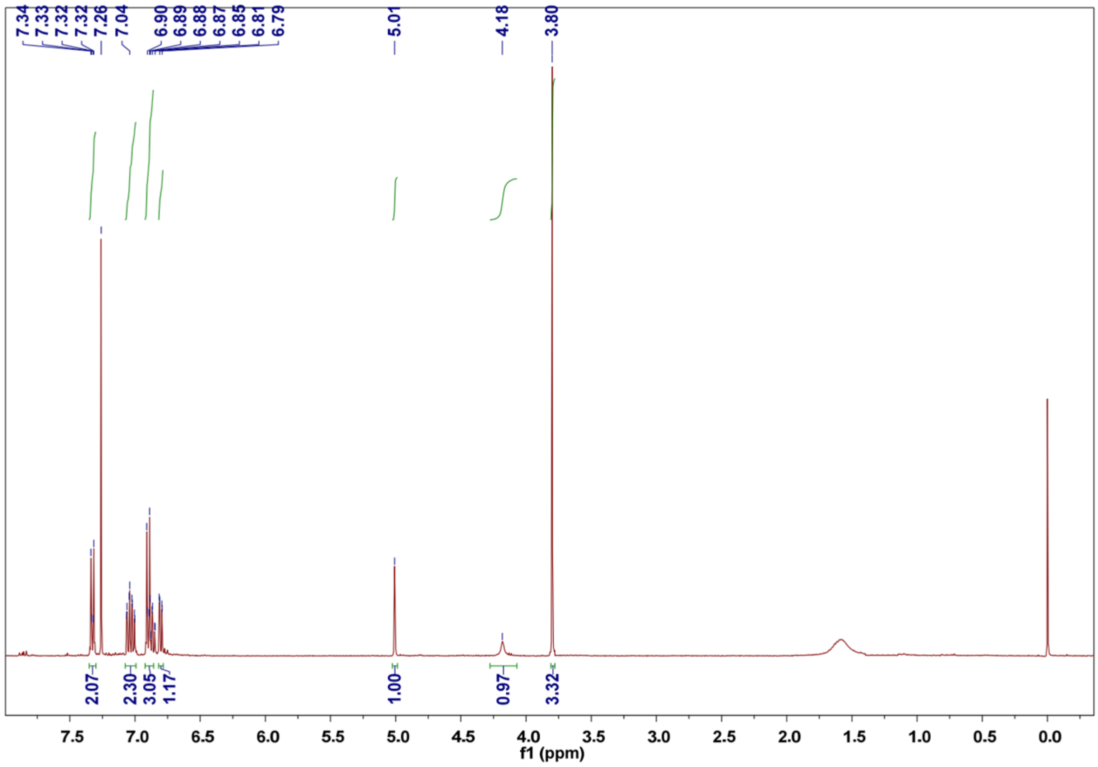

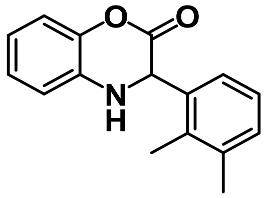

3-(2,3-dimethyphenyl)-3,4-dihydro-*2H*-benzo-1,4-oxazin-2-one: ^{1}H NMR (400 MHz, $CDCl_3$, *ppm*): δ 7.18 (s, 1H), 7.12 (s, 2H), 7.06-7.00 (m, 2H), 6.88-6.84 (m, 1H), 6.81-6.78 (m, 1H), 4.99 (s, 1H), 4.17 (s, 1H), 2.55 (s, 6H).

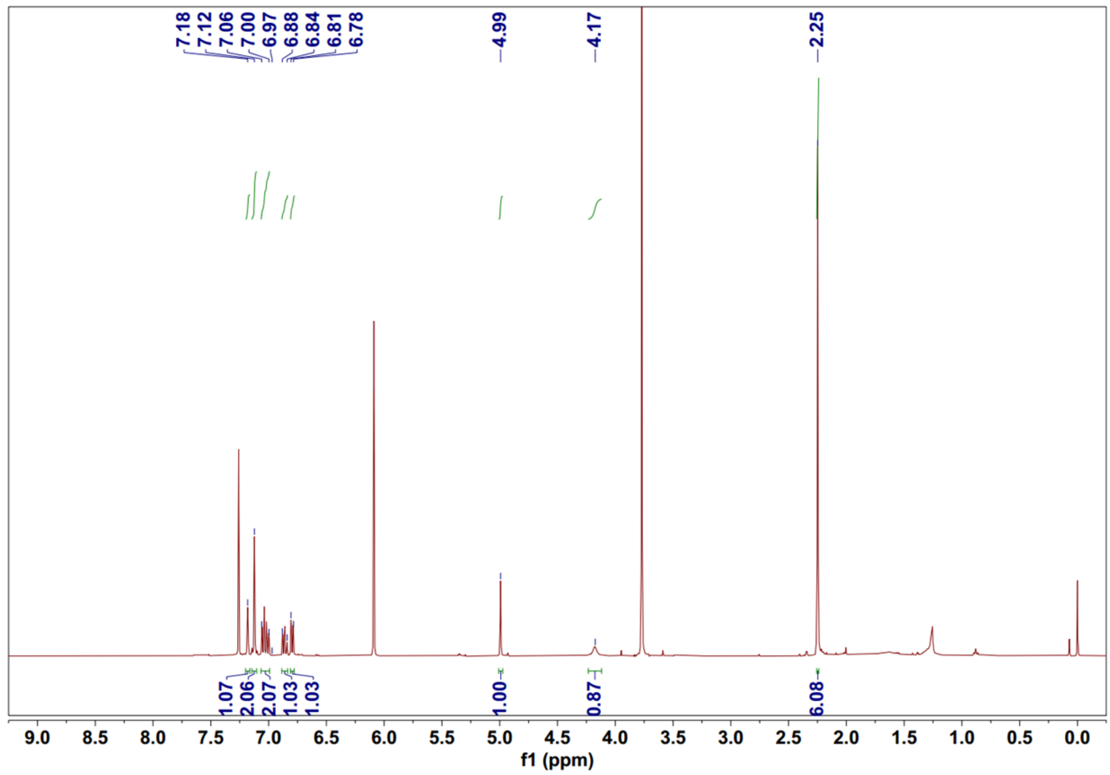

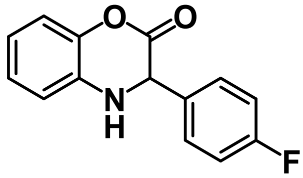

3-(4-fluorophenyl)-3,4-dihydro-*2H*-benzo-1,4-oxazin-2-one: ^{1}H NMR (400 MHz, $CDCl_3$, *ppm*): δ 7.42-7.36 (m, 2H), 7.09-7.02 (m, 4H), 6.91–6.86 (m, 1H), 6.84-6.82 (m, 1H), 5.05 (s, 1H).

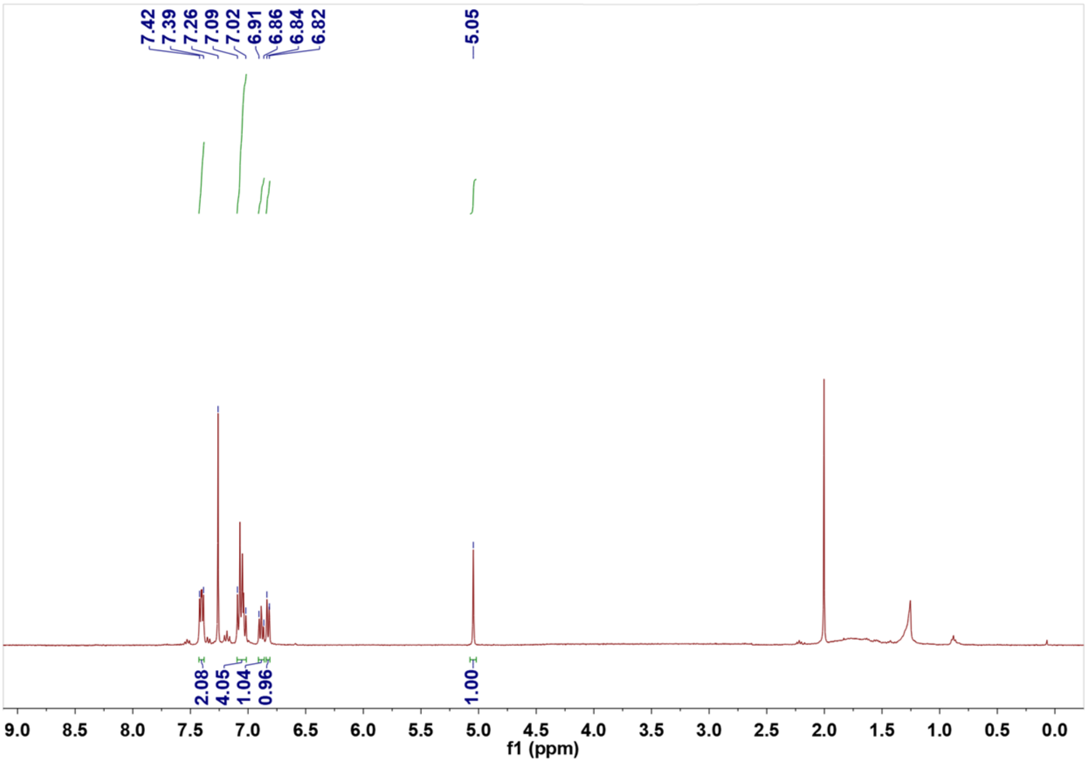

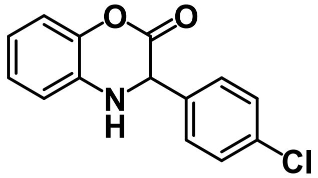

3-(4-chlorophenyl)-3,4-dihydro-*2H*-benzo-1,4-oxazin-2-one: [1]H NMR (400 MHz, $CDCl_3$, *ppm*): δ 7.36 (s, 4H), 7.17-7.12 (m, 2H), 7.01–6.97 (m, 1H), 6.94-6.92 (m, 1H), 5.15 (s, 1H).

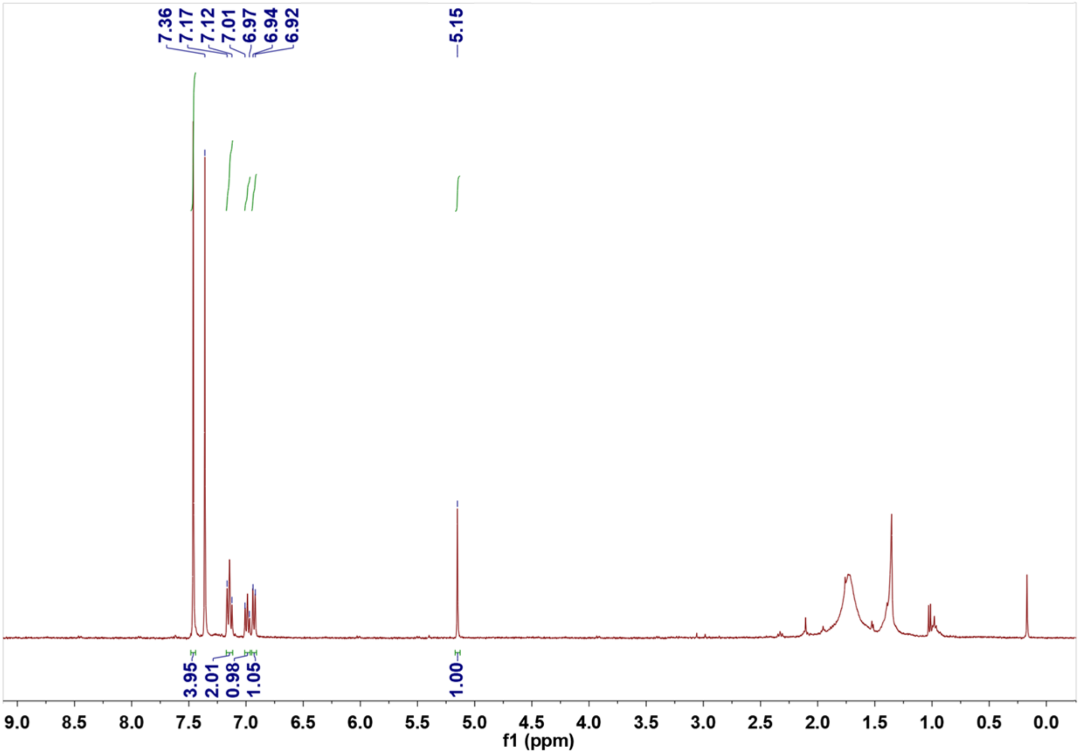

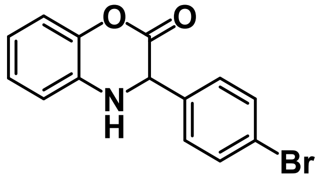

3-(4-bromophenyl)-3,4-dihydro-*2H*-benzo-1,4-oxazin-2-one: ^{1}H NMR (400 MHz, $CDCl_3$, *ppm*): δ 7.51 (d, *J* = 7.6, 2H), 7.30 (d, *J* = 7.6, 2H), 7.06-7.02 (m, 2H), 6.91-6.86 (m, 1H), 6.83 (d, *J* = 7.6, 1H), 5.03 (s, 1H).

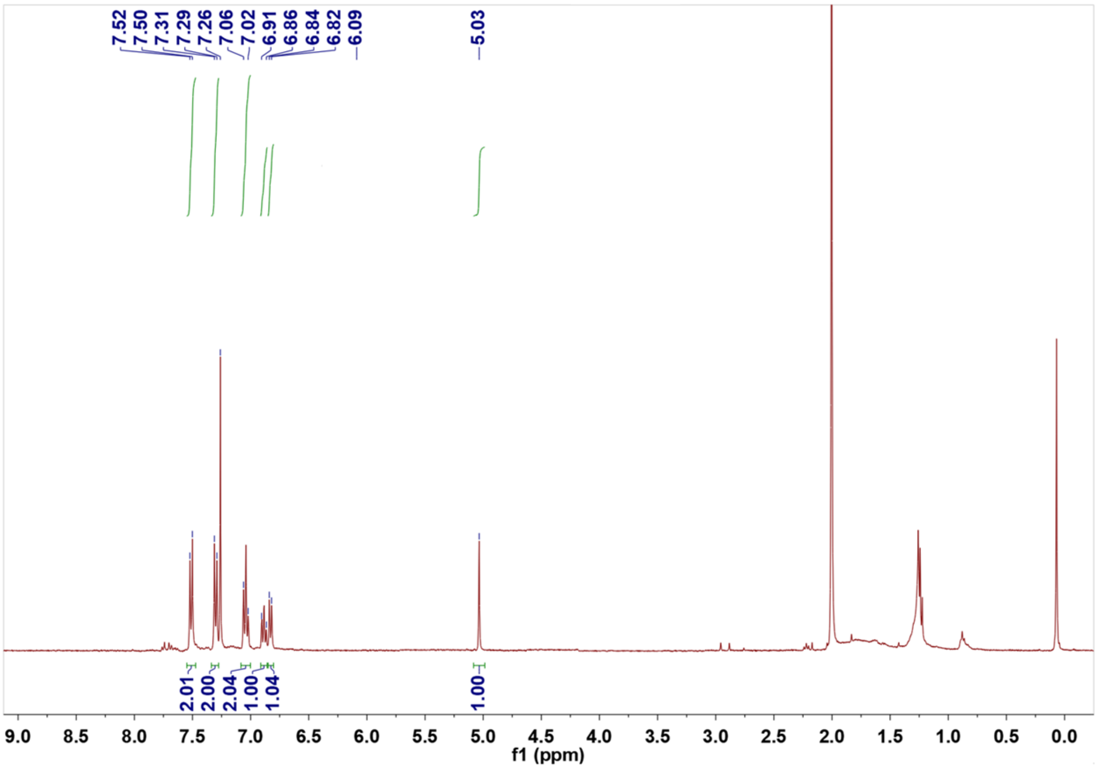

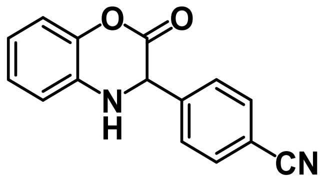

3-(4-nitrilephenyl)-3,4-dihydro-*2H*-benzo-1,4-oxazin-2-one: ^{1}H NMR (400 MHz, $CDCl_3$, *ppm*): δ 7.69 (d, *J* = 7.6, 2H), 7.57 (d, *J* = 7.6, 2H), 7.08-7.06 (m, 2H), 6.94-6.86 (m, 2H), 5.15 (s, 1H). 4.29 (s, 1H).

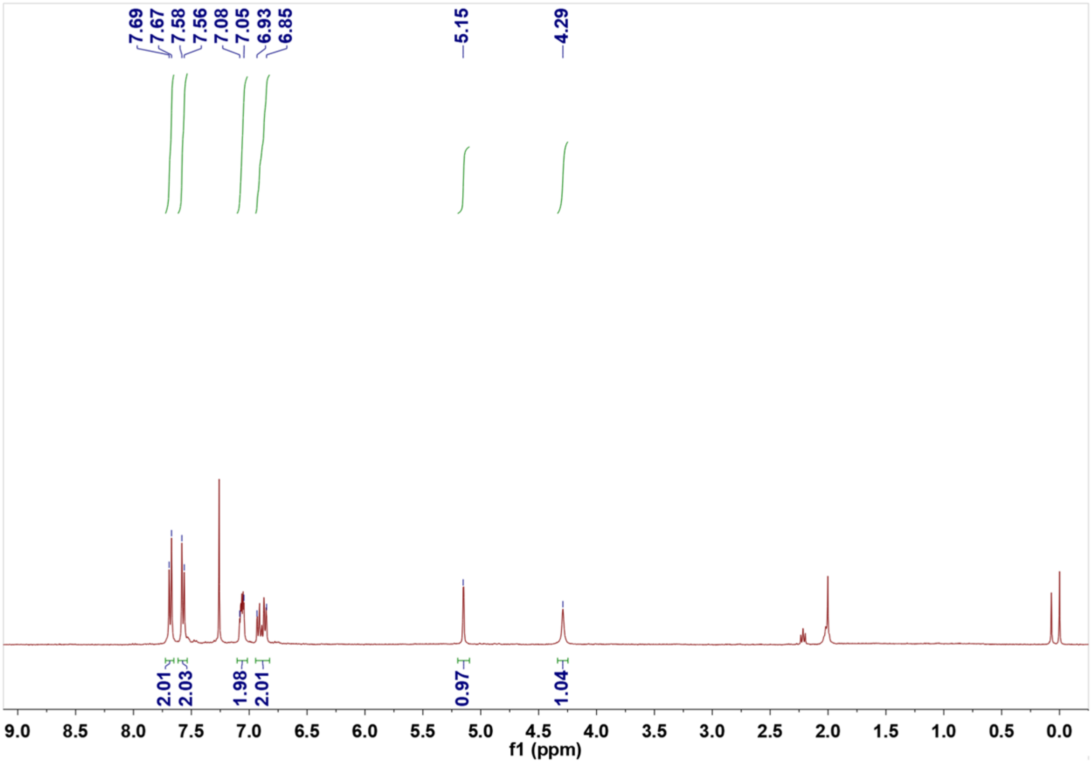

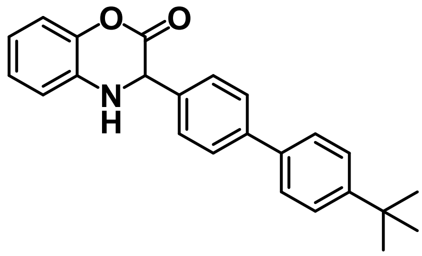

3-(4'-(*tert*-butyl)-[1,1'-biphenyl]-4-yl)-3,4-dihydro-*2H*-benzo-1,4-oxazin-2-one: [1]H NMR (400 MHz, $CDCl_3$, *ppm*): δ 7.59 (d, *J* = 8.0 Hz, 2H), 7.51 (d, *J* = 8.8 Hz, 2H), 7.48-7.45 (m, 4H), 7.09-7.02 (m, 2H), 6.90-6.82 (m, 2H), 5.11 (s, 1H), 4.26 (s, 1H), 1.36 (s, 9H).

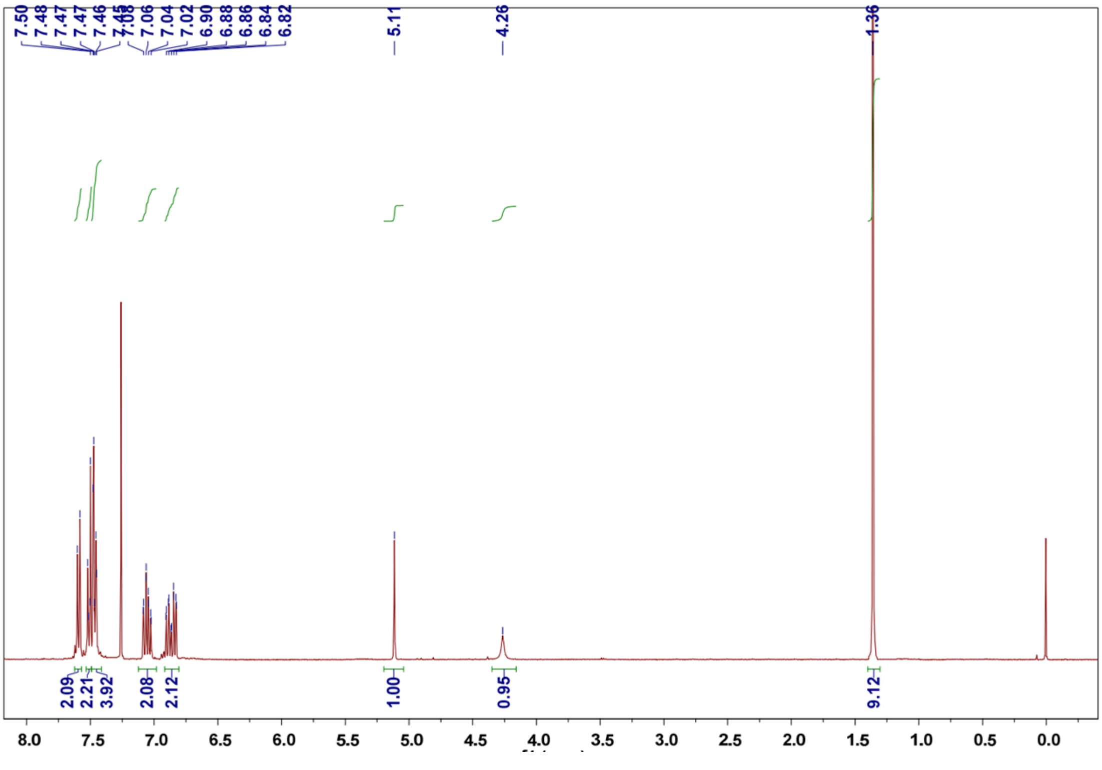

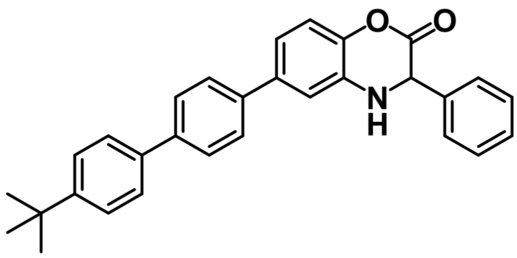

6-(4-(*tert*-butyl)phenyl)-3-phenyl-3,4-dihydro-*2H*-benzo-1,4-oxazin-2-one: [1]H NMR (400 MHz, $CDCl_3$, *ppm*): δ 7.48-7.43 (m, 6H), 7.39-7.36 (m, 3H), 7.09 (s, 2H), 7.02 (s, 1H), 5.12 (s, 1H), 4.32 (s, 1H), 1.36 (s, 9H).

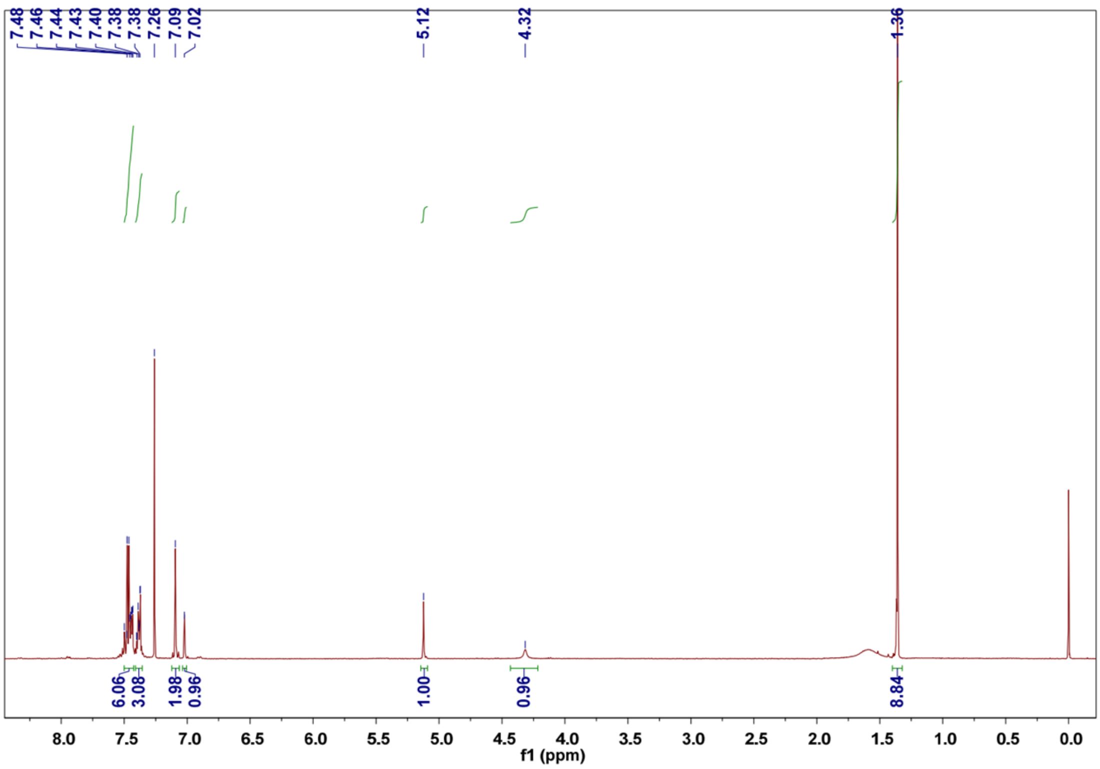

8. References

S1. Zhao, L.; Wei, J.-W.; Lu, J.-H.; He, C.; Duan, C.-Y. Renewable Molecular Flasks with NADH Models: Combination of Light-Driven Proton Reduction and Biomimetic Hydrogenation of Benzoxazinones. *Angew. Chem. Int. Ed.* **2017**, *56*, 8692-8696.

S2. Han Z.; Liu G.; Wang R.; Dong, X.-Q.; Zhang, X. Highly Efficient Ir-catalyzed Asymmetric Hydrogenation of Benzoxazinones and Derivatives with a Brønsted Acid Cocatalyst. *Chem. Sci.* **2019**, *10*, 4328-4333.

S3. SMART Data Collection Software, version 5.629; Bruker AXS Inc.: Madison, WI, 2003.

S4. SAINT Data Reduction Software, version 6.54; Bruker AXS Inc.: Madison, WI, 2003.

S5. Dolomanov, O. V.; Bourhis, L. J.; Gildea, R. J.; Howard, J. A. K.; Puschmann, H. OLEX2: A Complete Structure Solution, Refinement and Analysis Program. *J. Appl. Crystallogr*. **2009**, *42*, 339−341.

S6. Sheldrick, G. M. Crystal Structure Refinement with SHELXL. *Acta. Crystallogr. C Struct. Chem.* **2015**, *71*, 3−8.

S7. Sheldrick, G. M. SHELXT - Integrated Space-Group and Crystal-Structure Determination. *Acta. Crystallogr. A Found. Adv*, **2015**, *71*, 3−8.

S8. Spek, A. L. Single-Crystal Structure Validation with the Program *PLATON. J. Appl. Cryst.,* **2003**. *36*, 7−13.